AD-A115 576 AIR FORCE INST OF TECH WRIGHT-PATTERSON AFB OH SCHOO--ETC F/G 20/5
METHODS FOR AN ALTERNATING BEAM RING LASER.(U)
DEC 81 M L DRAKE
UNCLASSIFIED AFIT/GE/EE/81D-17 NL

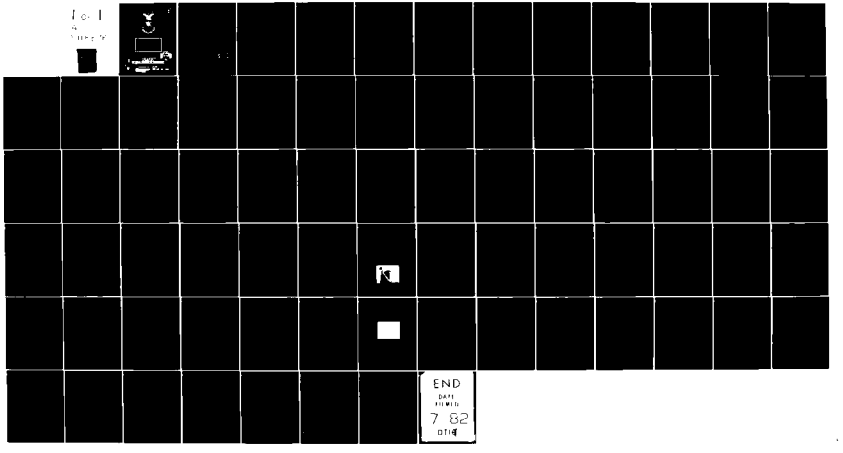

END
DATE FILMED
7 82
DTIC

AFIT/GE/EE/81*D-17

(1)

METHODS FOR AN ALTERNATING BEAM RING LASER

THESIS

AFIT/GE/EE/81*D-17 Marc L. Drake
2Lt USAF

AFIT/GE*/EE/81D-17

METHODS FOR AN ALTERNATING BEAM RING LASER

THESIS

Presented to the Faculty of the School of Engineering
of the Air Force Institute of Technology

Air University

In Partial Fullfillment of the
Requirements for the Degree of
Master of Science

by
Marc L. Drake
2Lt USAF
Graduate Electrical Engineering
December 1981

PREFACE

The purpose of this research is to investigate the feasibility of three methods of alternating beams in ring lasers. This study should serve as a basis for further investigations into this area.

My thanks are extended to Major Salvatore Balsamo for suggesting this area of research to me and for providing me with the necessary background knowledge and guidance during my studies. I also thank Mr. Robert McAdory of the Air Force Armament Development and Test Center, Eglin AFB, Florida for sponsoring this thesis. Also, thanks are extended to Mr. Carl Shortt and his personnel at the Model Fabrication Shop, and to Mr. Robert Durham and the personnel of the AFIT Electrical Engineering Laboratory for providing me with the fabricated components and other assistance necessary to complete my research work. Special thanks are given to Mrs. Vicki Francis for her excellent typing. Finally, I thank my family for their support and understanding during this period.

Table of Contents

Page

List of Figures

List of Tables

List of Symbols

c	Speed of light
C	Capacitance
CCW	Counter-clockwise
CW	Clockwise
d	Distance, thickness
E	Electric field
f	Focal length
g	g Parameter
H_a	Applied magnetic field
i	Current
I	Current
$\underline{k}_i$	Incident propagation vector
$\underline{k}_r$	Reflected propagation vector
$\underline{k}_t$	Transmitted propagation vector
K_λ	Fraction of a wavelength
K	Kerr constant
l	Length
L_c	Cavity length
L	Inductance
M	Internal magnetization
$\underline{n}$	Surface normal vector
n_e	Extraordinary ray refractive index
n_o	Ordinary ray refractive index
N	Number of coil turns

q	Integer
R	Resistance
R_i	Radius of curvature
R'_i	Corrected radius for curvature
v_z	Velocity along optic axis
V	Verdet constant
V_s	Voltage
Y	Admittance
z	Distance along optic axis
Z	Impedance
δ	Phase retardation
θ	Angle of incidence
θ_B	Brewster angle
θ_F	Faraday rotation
λ	Wavelength
μ	Mean
μ_o	Permeability of air
ν	Frequency
ν_c	Cavity frequency
ν_o	Emission center frequency
$\Delta\nu$	Longitudinal mode separation
σ	1 Standard deviation
ϕ	Optical phase difference
ω	Radian frequency
ω_o	Waist size
$\omega(z)$	Spot size

Abstract

The purpose of this research is to investigate the feasibility of three methods of alternating beams in ring lasers. The first method is the use of a Faraday cell and a half-wave plate inside the laser cavity to rotate the plane of polarization of one of the counter-rotating beams so that lasing in that direction is not supported. The second method, and the one investigated experimentally, is the use of mirrors and a mechanical chopper external to the laser cavity to halt lasing by means of mode competition. The third and final method explored is the replacement of the mechanical chopper with an electro-optical shutter.

METHODS FOR AN ALTERNATING BEAM RING LASER

I. Introduction

Background

The ring laser is a bi-directional traveling-wave device. There have been experiments done in the past few years to develop unidirectional lasers by use of optical isolators (Ref 1:544, 5:1371). This type of isolator allows lasing in one continual direction. There may be instances, however, where it is desirable to alternate the direction in which lasing occurs. One case in which this might be desirable is the use of the ring laser as a rotation sensor. This study will look at three possible methods of producing beam alternation.

Problem Statement

The purpose of this research is to investigate the feasibility of three methods of alternating beams in ring lasers. The first method is to use a Faraday cell and a half-wave plate inside the laser cavity to rotate the beam traveling in one direction or the other so that lasing in that direction is not supported. There is a disadvantage to this in that since the elements used in this method are

inside the cavity, slight misalignments may cause sufficient losses to stop lasing.

The second method considered, and the one which will be investigated experimentally, is the use of mirrors and a mechanical chopper external to the laser cavity to halt lasing by means of mode competition. The third and final method explored will be the replacement of the mechanical chopper of the second method with an electro-optical shutter. These last two methods have an advantage over the Faraday cell method in that they do not require that anything be placed in the laser cavity.

Method of Approach

The method of approach starts with literature research into the Faraday cell and mode competion methods of beam alternation. This is followed by an analysis of the three methods.

The next step is the design and construction of the ring laser cavity. This includes calculation of the beam dimensions and determination of cavity stability. Following this is the design and fabrication of the mechanical chopper and ancillary equipment. After fabrication, the chopper is installed and aligned so as to pass one beam while interrupting the other. The chopper experiment is then performed, and the results are recorded.

Order of Presentation

A description and results of the research are presented in the following manner. First, the theory of ring laser, Brewster windows, Faraday effect, mode competition, mechanical chopper, and electro-optic shutter are presented in Chapter II. This is followed by a discussion of the equipment design in Chapter III. The results of the experiment are presented in Chapter IV. Finally, conclusions and recommendations are made in Chapter V.

II. Theory

Ring Laser

The theory of ring lasers is basically that of the linear laser with the distinction that in the ring laser the number of degrees of freedom of the system are doubled. The reason for this is that while the linear laser has cavity modes consisting of two equal but oppositely directed traveling waves composing a standing wave, the ring laser traveling waves are independent. While they are still oppositely directed, they are free to oscillate with different amplitudes and frequencies.

The output frequency of the laser is a function of the optical cavity length. For resonance to occur, the length of a ring laser cavity must be equal to an integral number of wavelengths. This can be expressed as

$$q\lambda = L_c \tag{2.1}$$

or, since $\lambda\nu = c$

$$\nu = qc/L_c \tag{2.2}$$

where λ is the wavelength, ν is the resonant frequency, q is an integer, c is the speed of light, and L_c is the optical cavity length.

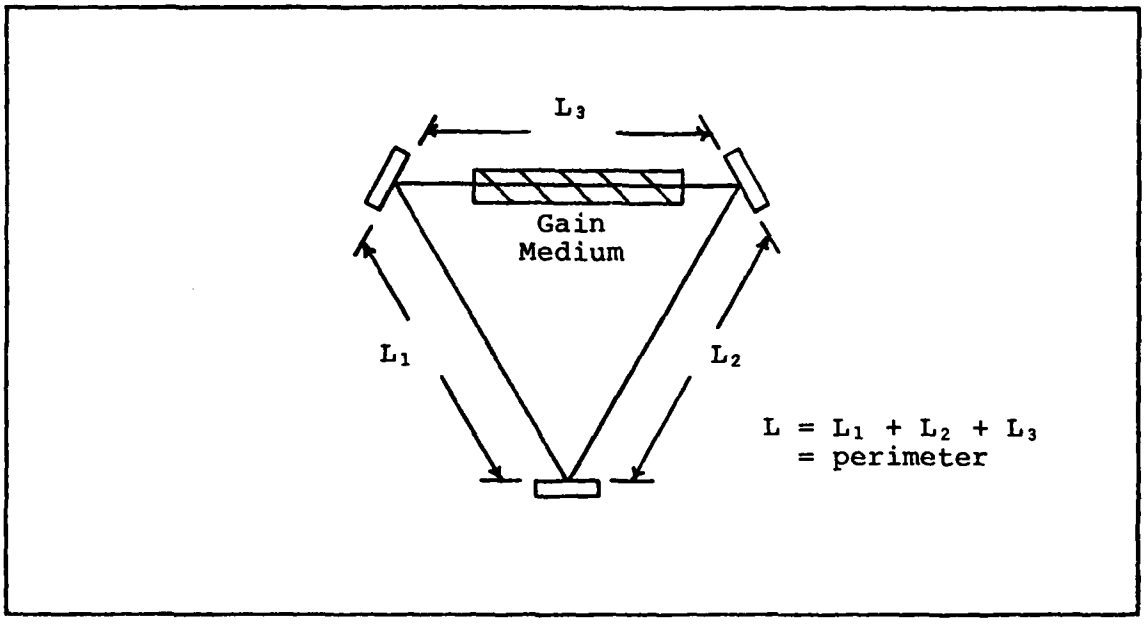

Figure 2.1 Ring Laser Cavity Configuration

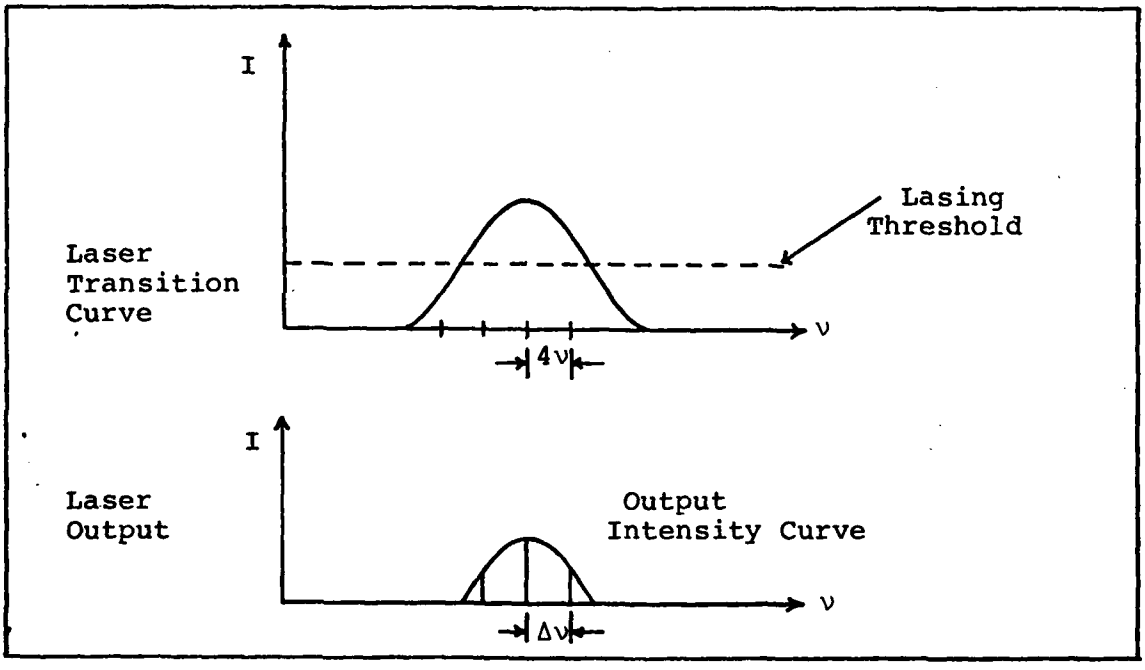

Figure 2.2 Relationship Between a Doppler Broadened Gain Curve, Axial Mode Spacing, and Laser Output Intensity

Because q may be any integer, there are an infinite number of frequencies or longitudinal modes at which a laser may resonate as long as ν is within the intensity vs. frequency plot. The longitudinal mode separation, $\Delta\nu$, is represented by

$$\Delta\nu = c/L \qquad (2.3)$$

Figure 2.2 shows the relationship between laser intensity, longitudinal mode spacing and gain (Ref 8:92).

In a helium-neon laser, the atoms may be in motion with respect to the optic axis. In Figure 2.3, the density of atoms in the excited state as a function of the z, or optic axis, component of the velocity is shown. Now assume a single longitudinal mode ring laser with a cavity mode frequency which is greater than the emission center frequency of the excited atoms, ν_o. The light in the cavity, as has been shown, is made up of two sets of waves, with one set traveling in the positive z direction and the other in the negative z direction. These waves are both at the cavity frequency ν_c. Those atoms which have no velocity component along the z axis will not be stimulated since the laser frequency is not at the emission center frequency. However, the atoms with a positive z axis velocity that satisifies the Doppler relationship

$$\nu_o = \nu_c\left(1 + \frac{V_z}{c}\right)^{-1}, \quad \nu_c > \nu_o \qquad (2.4)$$

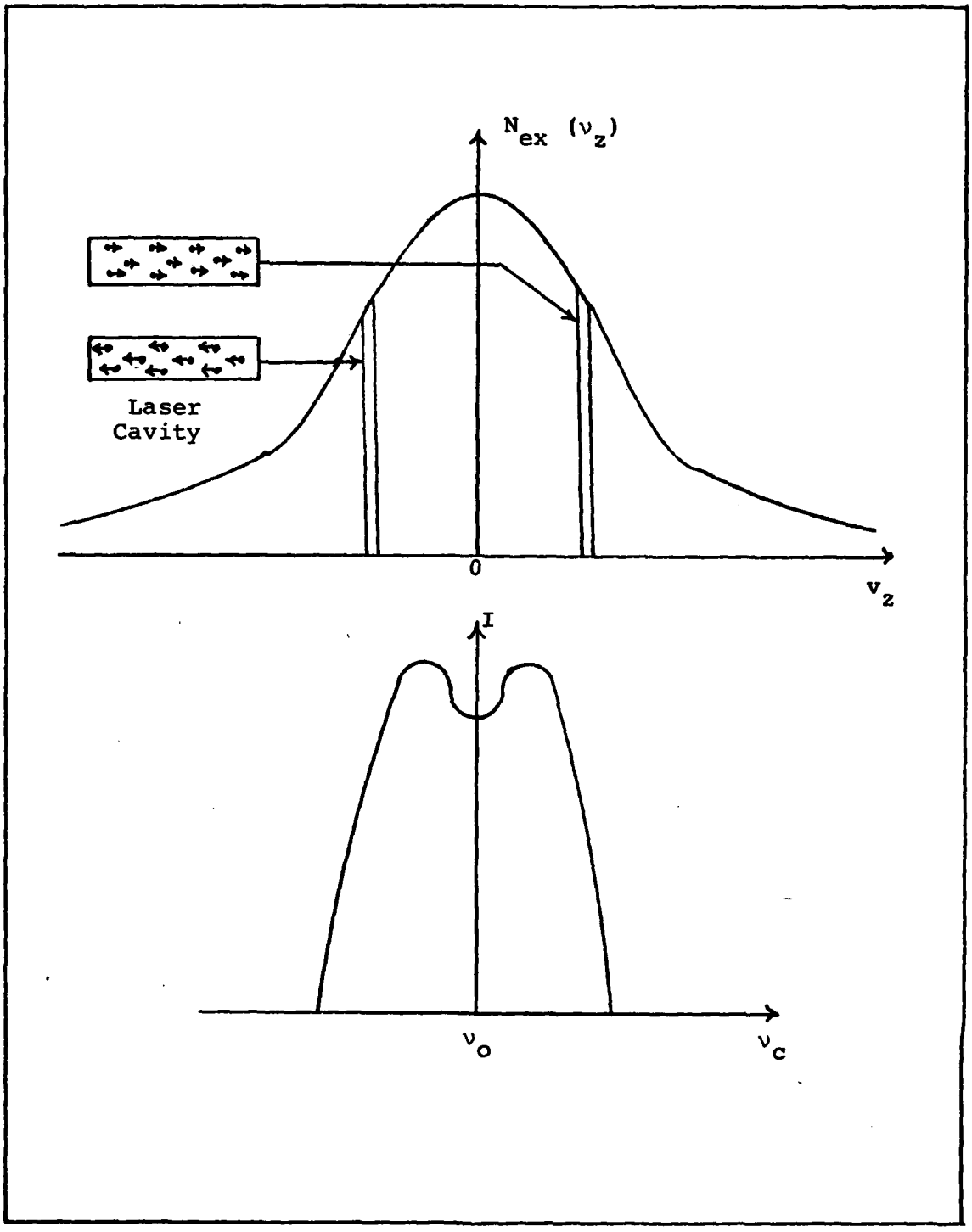

Figure 2.3 Distribution of Excited State Atoms Versus Z-Axis Velocity and Output of a Single Mode Laser as a Function of Cavity Frequency. The Minimum at the Center of the Curve Curve is the Lamb Dip

where c is the speed of light, will be stimulated. To this group of atoms, the frequency of the waves traveling in the positive z direction appears to be ν_o, and the atoms are stimulated to emit. The same occurs for atoms and waves which are moving in the negative z direction. This means that there are two groups of atoms which provide gain for the laser. In the case where the cavity frequency is the atomic resonance frequency, only a single group of atoms, those with no velocity along the optic axis, provides gain for the laser. When this occurs, laser output power drops, since fewer atoms are providing gain. If the laser output is plotted as a function of ν_c, as in Figure 2.3, there is a dip known as the Lamb dip at ν_o (Ref 8:112).

Brewster Windows

In order to obtain beam alternation by the methods considered in this discussion, it is necessary that the output of the laser be linearly polarized. This is achieved by the use of a gain tube with Brewster windows. It is possible by this method to achieve a ratio of 1000:1 between light polarized in one direction and that polarized in the orthogonal direction (Ref 8:46).

Brewster windows provide polarization by reflection. Light with its polarization vector parallel to a reflecting surface is preferentially reflected, as shown in Figure 2.4. This figure shows randomly polarized light resolved

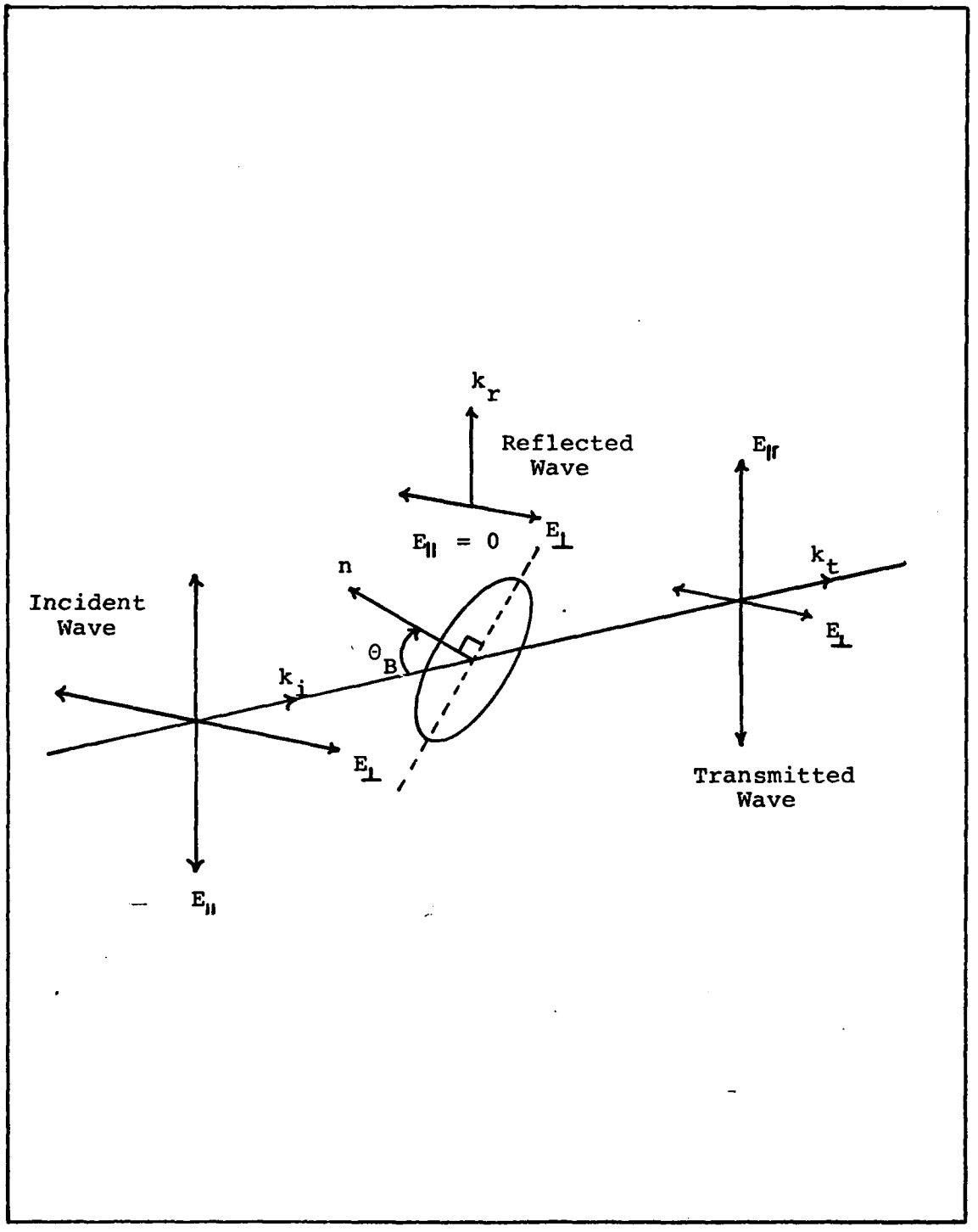

Figure 2.4 Polarization by Reflection

into two vectors, perpendicular to one another and of equal length. They are normal to the incident propagation vector $\underline{k}_i$. Also shown are the transmitted ($\underline{k}_t$) and reflected ($\underline{k}_r$) waves at an angle Θ to the surface normal, $\underline{n}$. The plane of incidence is the plane which contains both $\underline{n}$ and $\underline{k}_i$. The electric fields are labeled according to their orientation with respect to the plane of incidence. For normal incidence ($\Theta = 0$), equal amounts of light in all polarizations are reflected at the surface. For increasing angles of incidence, less of the light polarized parallel to the plane of incidence is reflected, while more is transmitted. When Θ reachs Θ_B, which is known as the Brewster angle, the refractive indices of the two media forming the surface are such that all light that is polarized parallel to the plane of incidence is transmitted. This angle is related to the refractive indices of the two media by

$$\Theta_B = \tan^{-1} \left(\frac{n_2}{n_1}\right) \qquad (2.5)$$

where n_1 is the medium of the incident light and n_2 is the refractive index of the medium into which the light is transmitted (Ref 8:43). Thus for light transmitted from air ($n \approx 1$) to glass ($n \approx 1.5$) a value of $\Theta_B \approx 56.3$ degrees is obtained. Figure 2.5 (Ref 3:10-82) shows the reflectance of light polarized parallel and perpendicular to the plane of incidence as a function of angle of incidence.

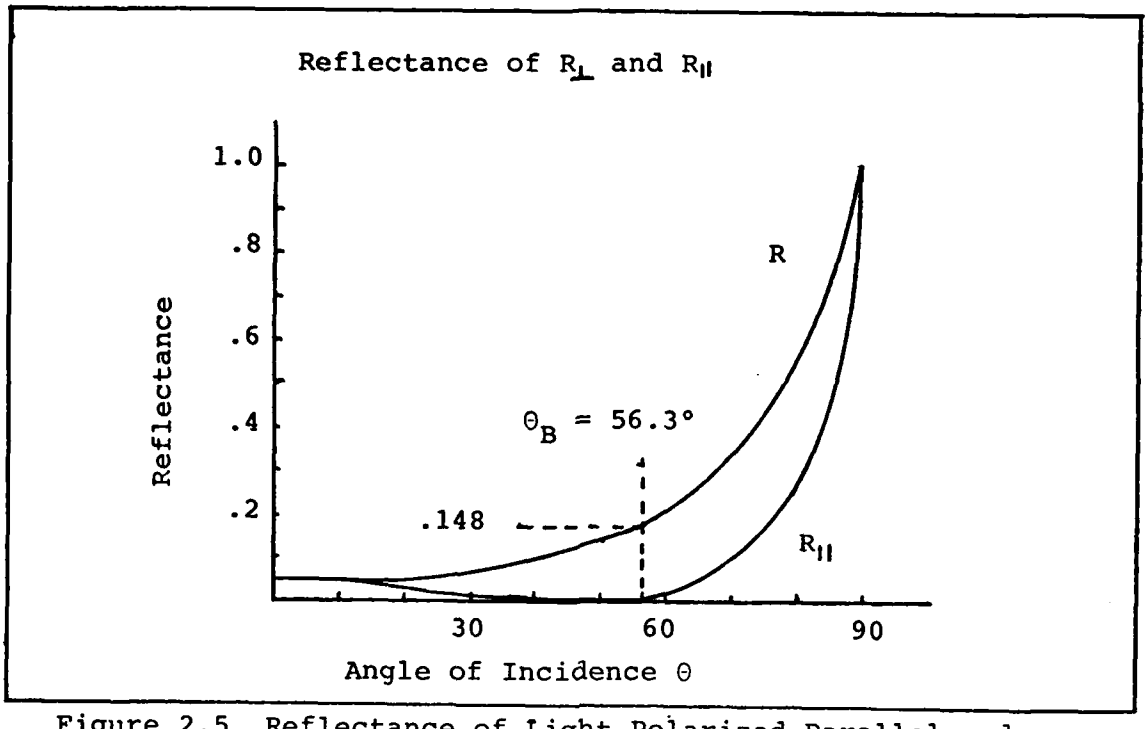

Figure 2.5 Reflectance of Light Polarized Parallel and Perpendicular to the Plane of Incidence as a Function of Angle of Incidence for n = 1.5

Faraday Effect

The Faraday effect is one of two first order magneto-optic effects. Magneto-optic effects are modifications of optical beam parameters caused by transmission through or reflection from a material medium to which an external magnetic field H_a has been applied or in which a magnetization M exists (Ref 4:9). The Faraday effect occurs upon transmission through the medium, the Kerr effect, with which we will not be concerned, occurs upon reflection from the medium.

The Faraday effect is a rotation of the plane of polarization of plane polarized light through an angle

when transmitted through a medium in a direction parallel to an externally applied magnetic field (Ref 6:17-20). This rotation is given by

$$\theta_F = V H_a d \qquad (2.6)$$

where V is the Verdet constant and d is the distance through the medium. The Verdet constant usually increases with the refractive index n (Ref 1:544). The direction of rotation of the polarization is the same as the direction of the current in the coil surrounding the transmission medium, as is shown in Figure 2.6.

As an example, assume a Faraday cell constructed from a 1,000 turn, 15 cm long solenoid, with a glass core of Verdet constant .0317 arc min/(Oe)(cm). Further assume a current of 10 A through the solenoid. Application of Ampere's Law

$$\oint \underline{H} \cdot dl = NI$$

produces a magnetic field of 6.67 X 10 A/m, or 837.8 Oe. When these numbers are inserted in Eq 2.5, it yields

$$\begin{aligned} \theta_F &= (.0317 \text{ min/Oe cm})(837.8 \text{ Oe})(15 \text{ cm}) \\ &= 398.3 \text{ min} \\ &= 6.64 \text{ degrees} \end{aligned}$$

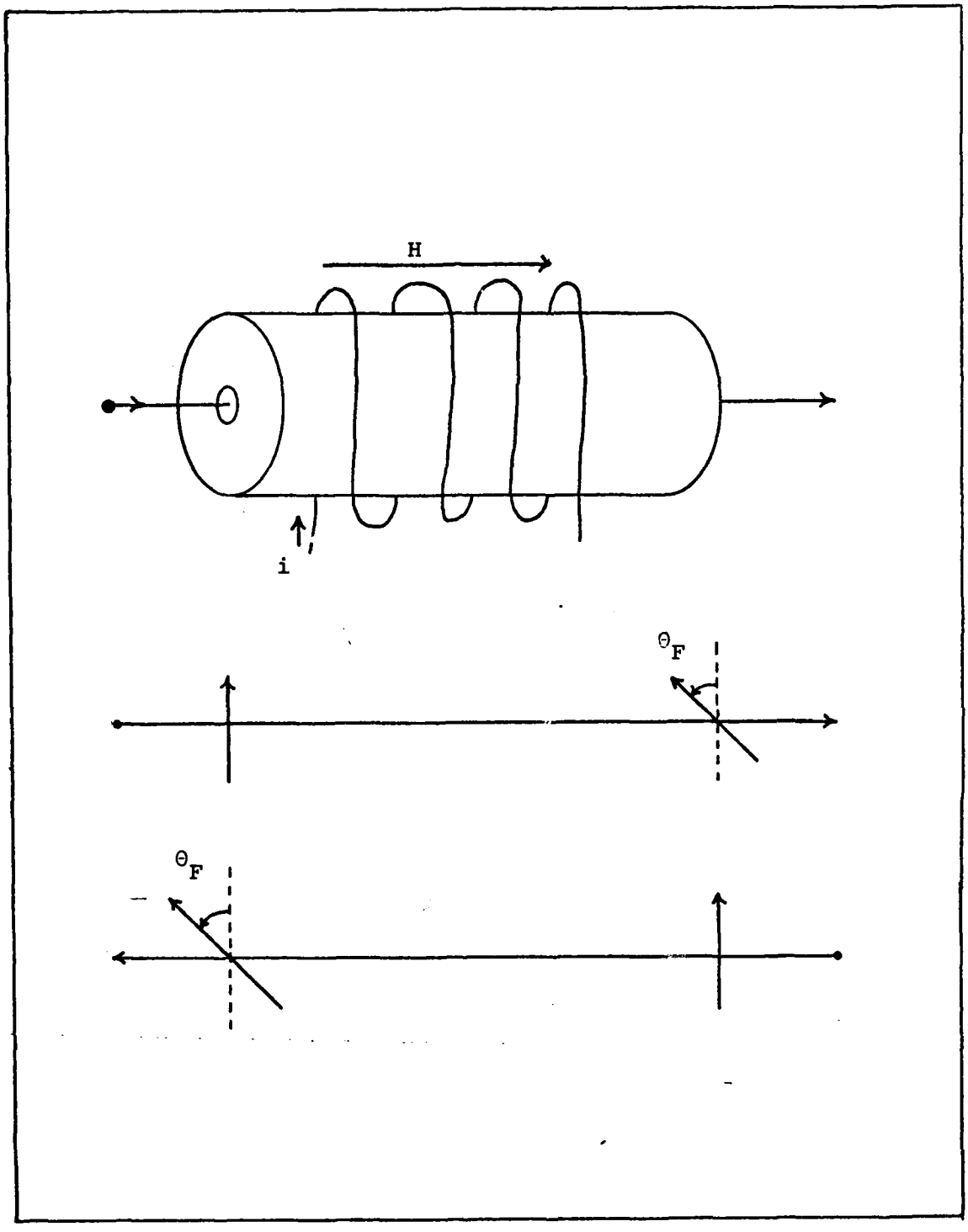

Figure 2.6 Faraday Cell and Resulting Beam Rotation

Retardation Plates

Retardation plates are constructed of birefringent uniaxial material in which the ordinary and extraordinary rays travel at different velocities. Because of this, one ray is retarded relative to the other, with the optical path difference $K\lambda$ between the two rays given by

$$K\lambda = \pm d\,(n_e - n_o) \qquad (2.7)$$

where K_λ is the retardation in fractions of a wavelength, λ is the wavelength, d is the physical thickness of the retardation plate, n_o is the refractive index of the ordinary ray, and n_e is the refractive index of the extraordinary ray. The positive and negative signs refer to negative and positive uniaxial crystal, positive for $n_e > n_o$, negative for $n_e < n_o$.

The phase difference between the two rays traveling through the birefringent material is $2\pi/\lambda$ times the path difference. Thus the phase retardation δ is obtained by multiplying Eq 2.7 by $2\pi/\lambda$, resulting in

$$\delta = \frac{2\pi}{\lambda} K\lambda = \pm \frac{2\pi}{\lambda} d(n_e - n_o)$$

$$\delta = 2\pi K_\lambda = \pm \frac{2\pi d(n_e - n_o)}{\lambda} \qquad (2.8)$$

It can then be seen that quarter-wave, half-wave, and three quarter-wave plates produce phase differences of $\pi/2$, π, and $3\pi/2$, respectively (Ref 3:10-102, 103).

Figure 2.8 shows the changes in polarization of a light wave after it passes through retardation plates of increasing thickness with the incident light polarized at an angle of 45 degrees to the fast axis of the plate. A retardation of $\lambda/8$ means that the ordinary and extraordinary waves are $\lambda/8$ out of phase with each other. This produces elliptically polarized light with the major axis of the ellipse coinciding with the axis of the original plane polarized beam. With an increase in retardation, the ellipse turns into a circle. For a retardation of $\lambda/4$ the transmitted beam is right circularly polarized. As retardation continues to increase, the transmitted light is elliptically polarized with the major axis of the ellipse at right angles to the fast axis of the plate, with the minor axis of the ellipse shrinking to zero, and producing plane polarized light at $\lambda/2$. Increasing the retardation further causes the patterns to change in the opposite order, with left circularly polarized light occuring at $3\lambda/4$. When retardation is full wave, the incident light passes through unchanged, although the slow wave is retarded by a full wavelength relative to the fast wave (Ref 3:10-104).

Because a half-wave plate is used in the Faraday cell optical switch, a closer look at its operation is warranted. Figure 2.9 shows light incident upon a half-wave plate with

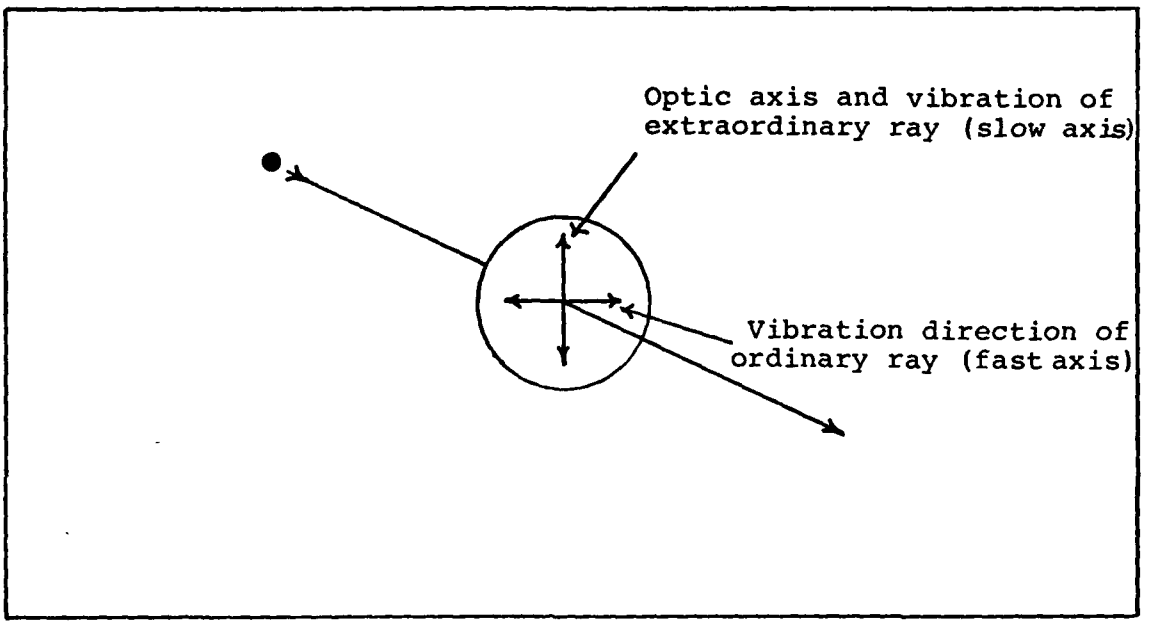

Figure 2.7 Light Incident Normally on the Front Surface of a Retardation Plate Showing the Vibration Directions of the Ordinary and Extraordinary Rays

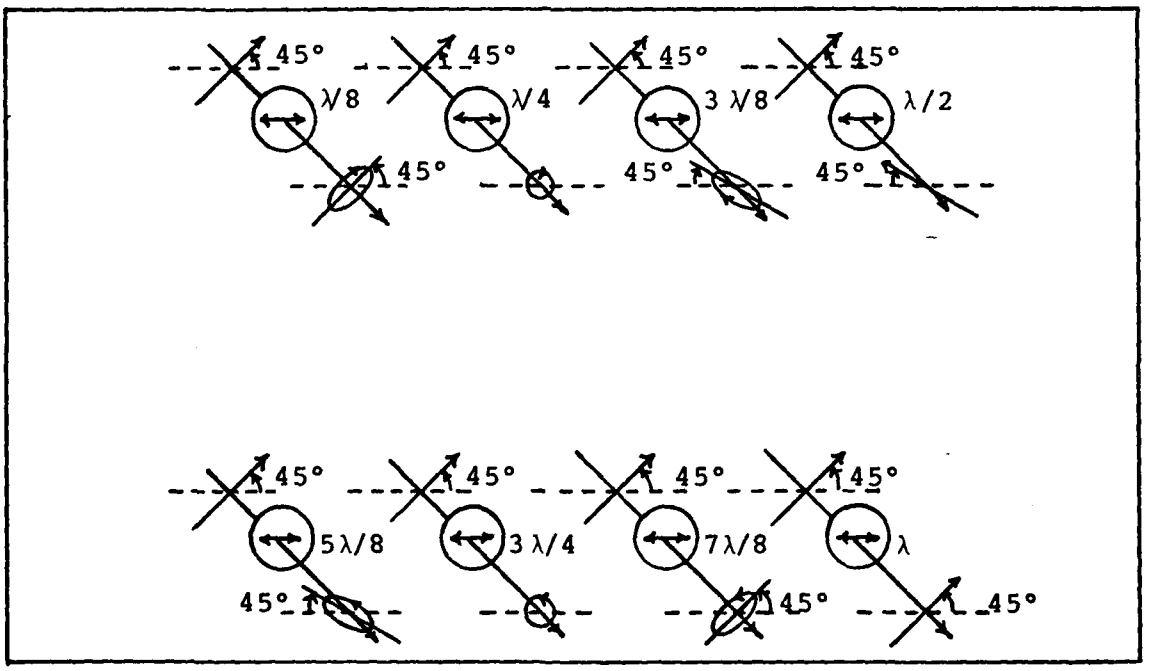

Figure 2.8 State of Polarization of a Light Wave after Passing Through a Retardation Plate (indicated in fractions of a wavelength). Incident Light is Polarized at 45° to the Fast Axis.

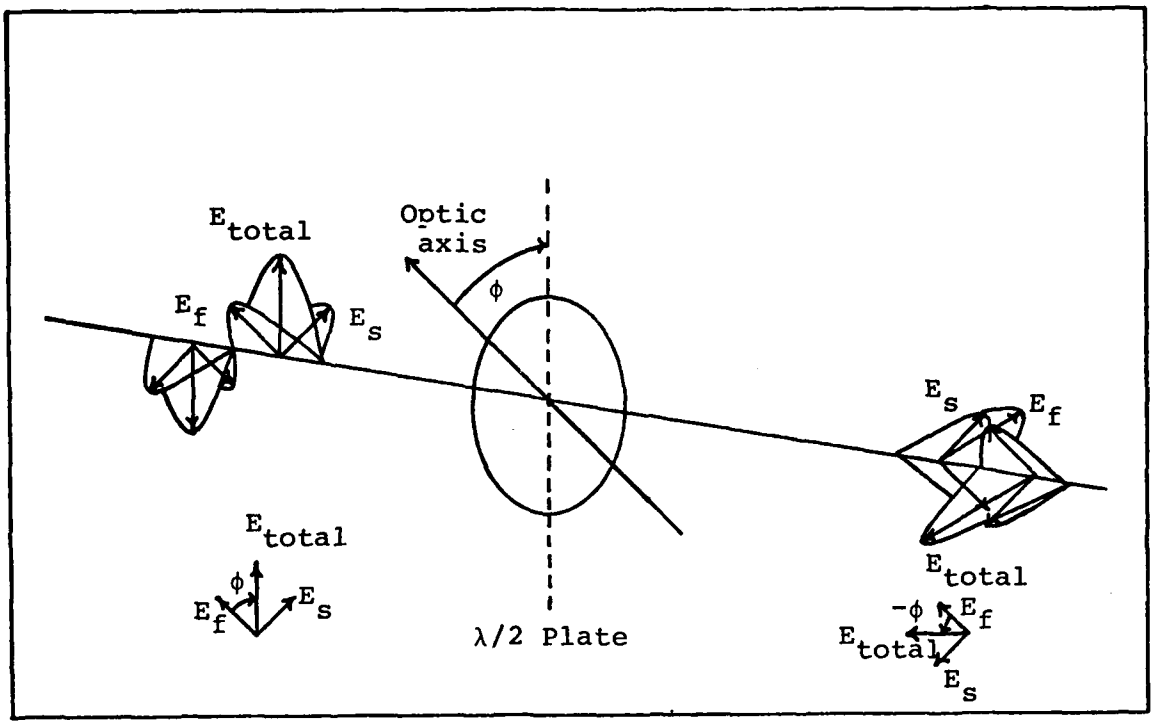

Figure 2.9 Half-wave Plate as a Polarization Rotator

its plane of polarization at an angle ϕ to the optic axis. After passing through the wave plate, the slow wave has been retarded a half-wave length, resulting in the rotation of the plane of polarization to an angle of $-\phi$ to the optic axis.

Faraday Cell Optical Switch

An optical switch may be constructed from a Faraday cell and a half-wave plate. The switch is introduced into the laser cavity with the half-wave plate aligned such that the plane polarized laser beam is incident upon it at an angle of 22.5 degrees with respect to the optic axis.

This arrangement is shown in Figures 2.10 and 2.11. This switch takes advantage of the Brewster windows of the laser gain tube. The Brewster windows allow lasing to occur only for light plane polarized in a single direction. This is due to the reflection of light polarized perpendicular to the plane of incidence, resulting in a large loss at the Brewster surface.

Using Figure 2.11 for illustration, the Brewster windows are assumed to allow lasing for light polarized in the vertical direction. The half-wave plate, as stated above, is oriented with its optic axis 22.5 degrees from the vertical. Vertically polarized light entering from the left is rotated 45 degrees clockwise. The light then passes to the Faraday cell, which is driven by current i to set up the magnetic field H in the direction shown. With H as shown, the light coming from the left is rotated a further 45 degrees clockwise, resulting in horizontally polarized light. This light will be reflected at the Brewster window, and lasing will not be sustained in this direction. Light entering from the right, however, first enters the Faraday cell. It is rotated 45 degrees clockwise (with respect to the direction of transmission). The half-wave plate then rotates it 45 degrees counter-clockwise, resulting in zero net rotation, allowing the ring to sustain lasing in that direction.

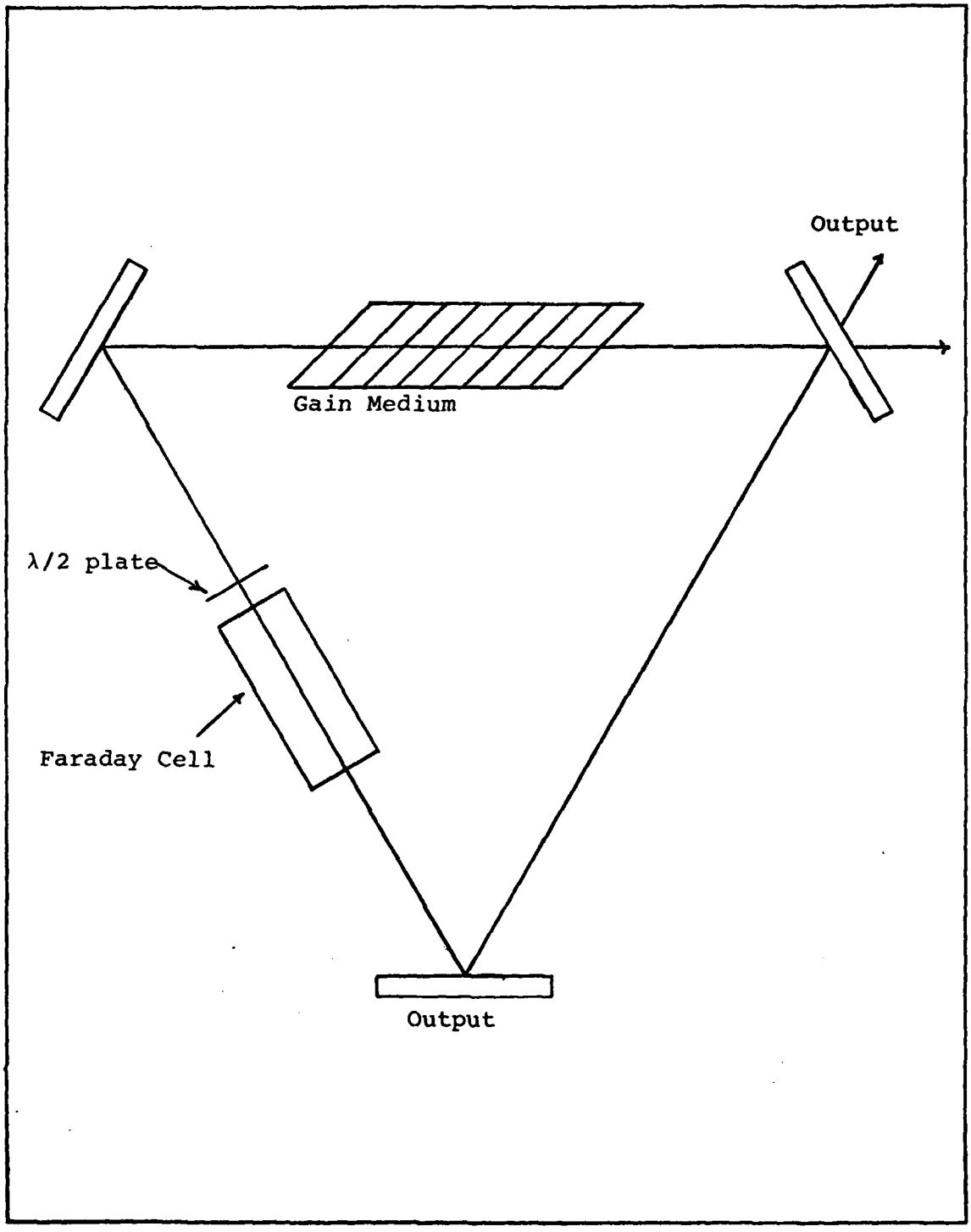

Figure 2.10 Laser Cavity With Faraday Cell Optical Switch

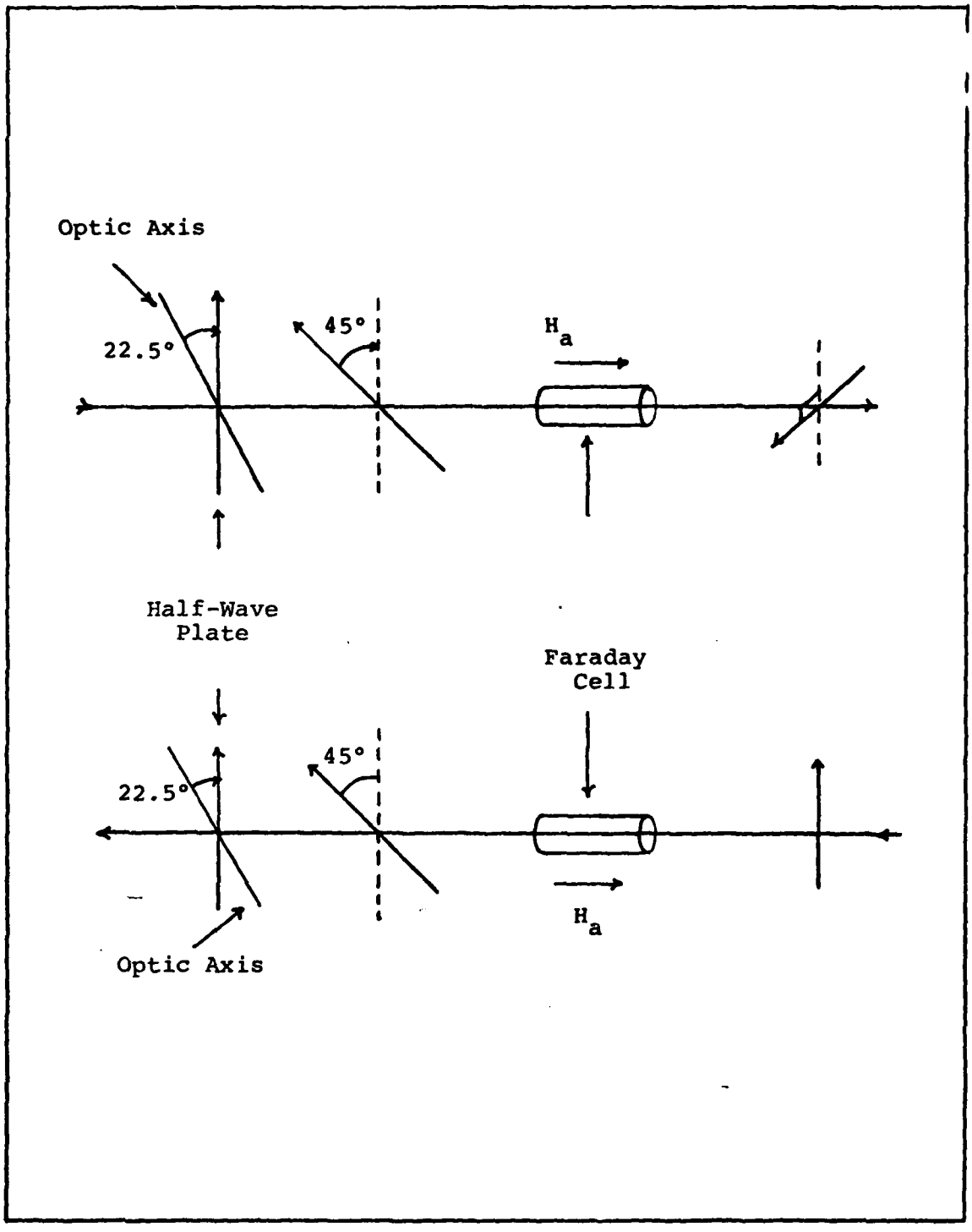

Figure 2.11 Faraday Cell Optical Switch Operation

By changing the direction of the current i, the magnetic field H is reversed. In this case, light entering from the left is rotated 45 degrees clockwise by the half-wave plate and is then rotated 45 degrees counter-clockwise by the Faraday cell, resulting in vertically polarized light. This now allows lasing in the direction to the right. Light entering from the right, traveling left, is rotated 45 degrees counter-clockwise by the Faraday cell, and then 135 degrees clockwise by the half-wave plate. This results in horizontally polarized light, and lasing in this direction is not sustained.

It should not be necessary to achieve a full 90 degree rotation of the plane of polarization of the laser beam to stop lasing. Using Figure 2.12 to illustrate, the lasing threshold on the intensity as a function of frequency plot is the level at which losses equal gain. Reflection at the Brewster window increases the losses, raising the lasing threshold level. Thus it is only necessary to increase the losses to the extent that there is no gain available to overcome them.

Since beam alternation would be achieved by the application of a square wave to the Faraday cell, the frequency response of the circuit will determine the rate at which the beams can be alternated. Figure 2.13 shows the Faraday cell circuit and the magnitude and phase plots of the admittance of the circuit as functions of frequency. As is shown, the circuit is a series RL circuit. Applying phasor

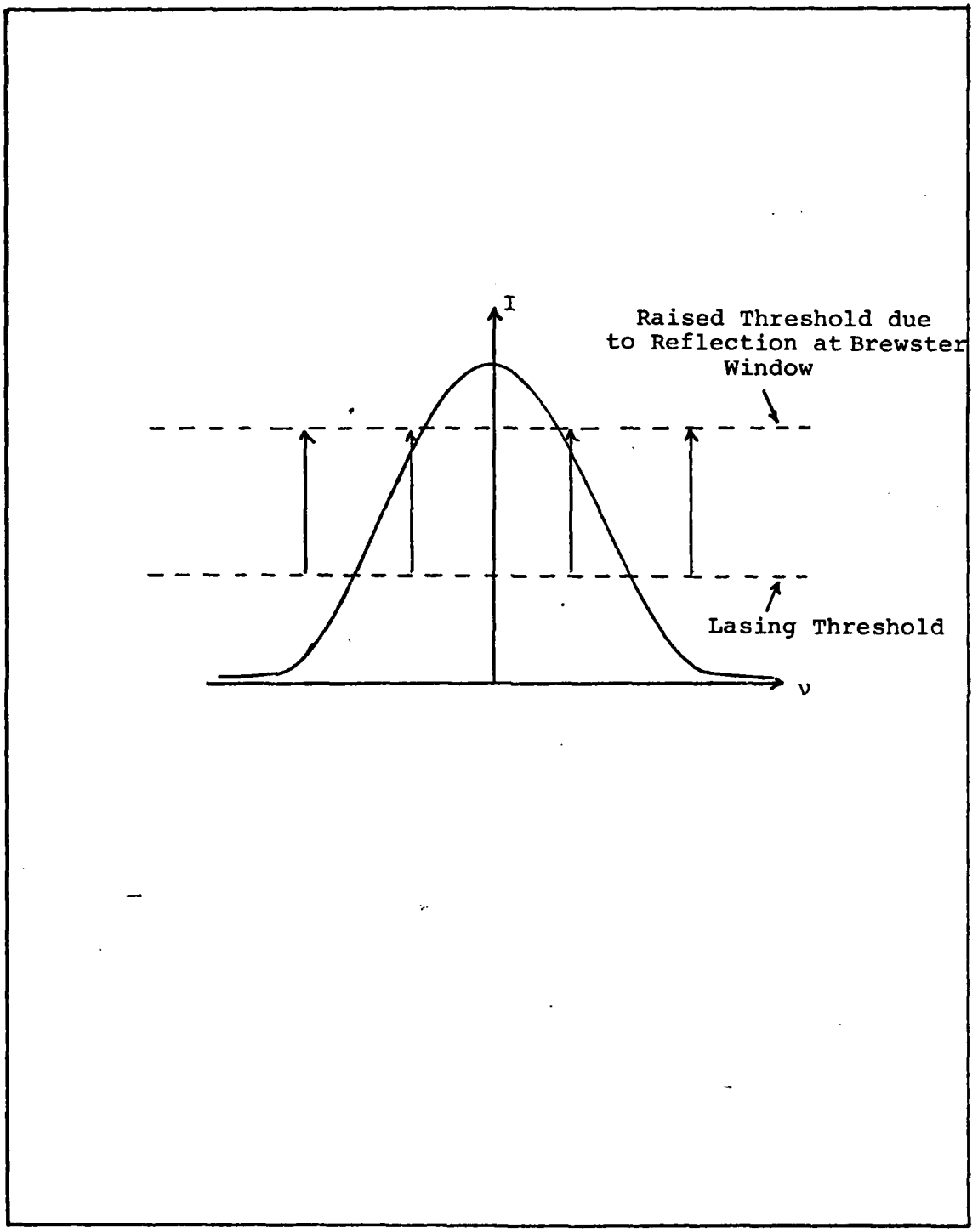

Figure 2.12 Raising of Lasing Threshold due to Reflection at Brewster Window Because of Faraday Switch Rotation

methods to the circuit, the phasor voltage $\underline{V}_s$ is applied to the circuit and the phasor current $\underline{I}$ is the desired response. The current $\underline{I}$ obtained is found to be

$$\underline{I} = \frac{\underline{V}_s}{R + j\omega L} \tag{2.9}$$

or expressed as admittance

$$\underline{Y} = \frac{\underline{I}}{\underline{V}_s} = \frac{1}{R + j\omega L} \tag{2.10}$$

The admittance may be considered to be the current produced by a source voltage $1\angle 0°$ V. The magnitude of the response is

$$|\underline{Y}| = \frac{1}{\sqrt{R^2 + \omega^2 L^2}} \tag{2.11}$$

with the angle of the response found as

$$\text{ang } \underline{Y} = -\tan^{-1}\frac{\omega L}{R} \tag{2.12}$$

These results are shown graphically in Figure 2.13.

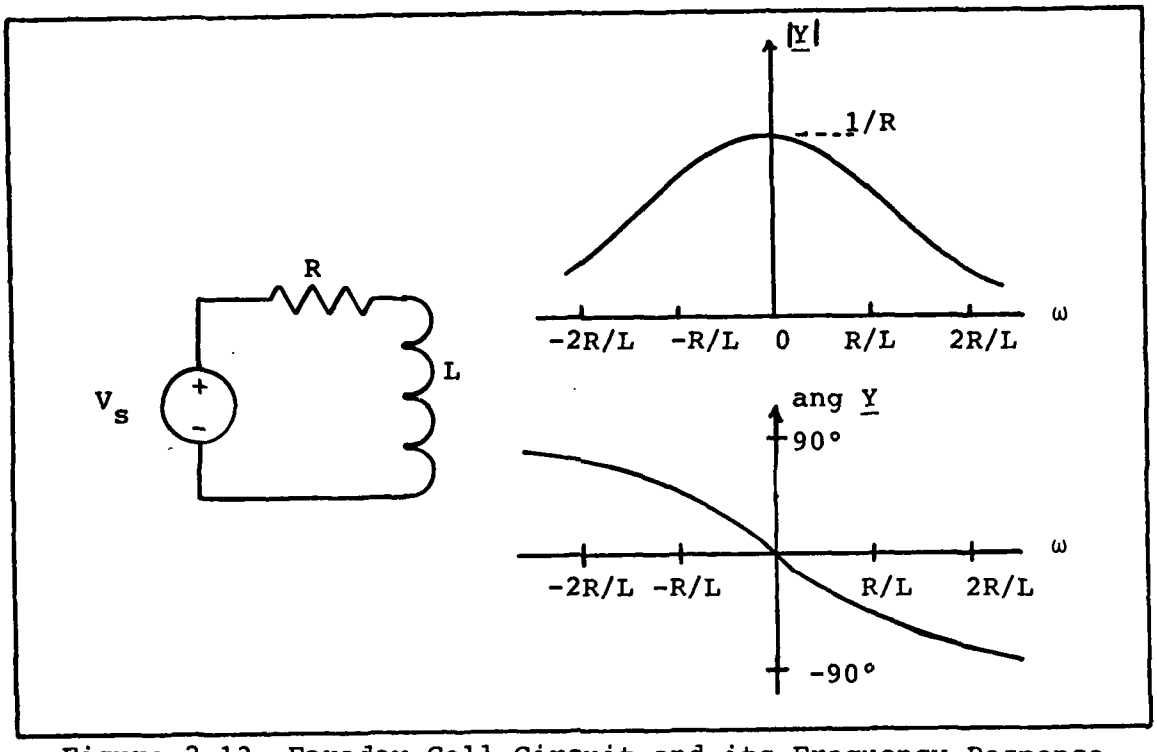

Figure 2.13 Faraday Cell Circuit and its Frequency Response

As an example, return to the 1,000 turn, 15 cm long coil used previously. Further assume that the coil has a radius of 1.5 cm, and that the output resistance of the voltage source is 600 Ω. The inductance of the coil may be found by

$$L = \frac{\mu N^2 A}{l}$$

where μ is $400\pi \times 10^{-9}$ Hm^{-1}, and A is the cross-sectional area of the coil. This gives an inductance of 5.92 mH for the coil. With a 600Ω source resistance and a 5.92 mH inductance, the half-power point of the response curve, $\omega = L/R$ is at 16.131 KHz.

Mode Competition

Two methods of producing beam alternation by means of mode competition are considered: first, the use of a mechanical shutter or chopper, and second, an electro-optic shutter.

Mode competition is an effect of a phenomenon known as gain saturation. Gain saturation is the pinning of the steady state gain at the threshold value for the gain medium. When gain saturation occurs, the gain of the cavity is equal to the losses. When a steady state condition exists in the gain medium, the population inversion, that is, the condition where the population of atoms in the excited state exceeds the population of atoms in the rest state, is at equilibrium (Ref 8:99). When this equilibrium exists, there are only sufficient excited atoms to sustain lasing at the steady state level.

To make use of this condition in the production of beam alternation, two mirrors are placed external to the laser cavity such that they reflect both the clockwise (CW) and the counter-clockwise(CCW) beams back into the cavity, as in Figure 2.14. Using the CW beam as an example, the reflected beam, being exactly the same frequency as the CW beam, will be competing for the same gain atoms as the CW beam. Since the population of gain atoms is fixed due to gain saturation, a reduction in the gain available for sustaining the CW beam occurs. By causing a sufficient

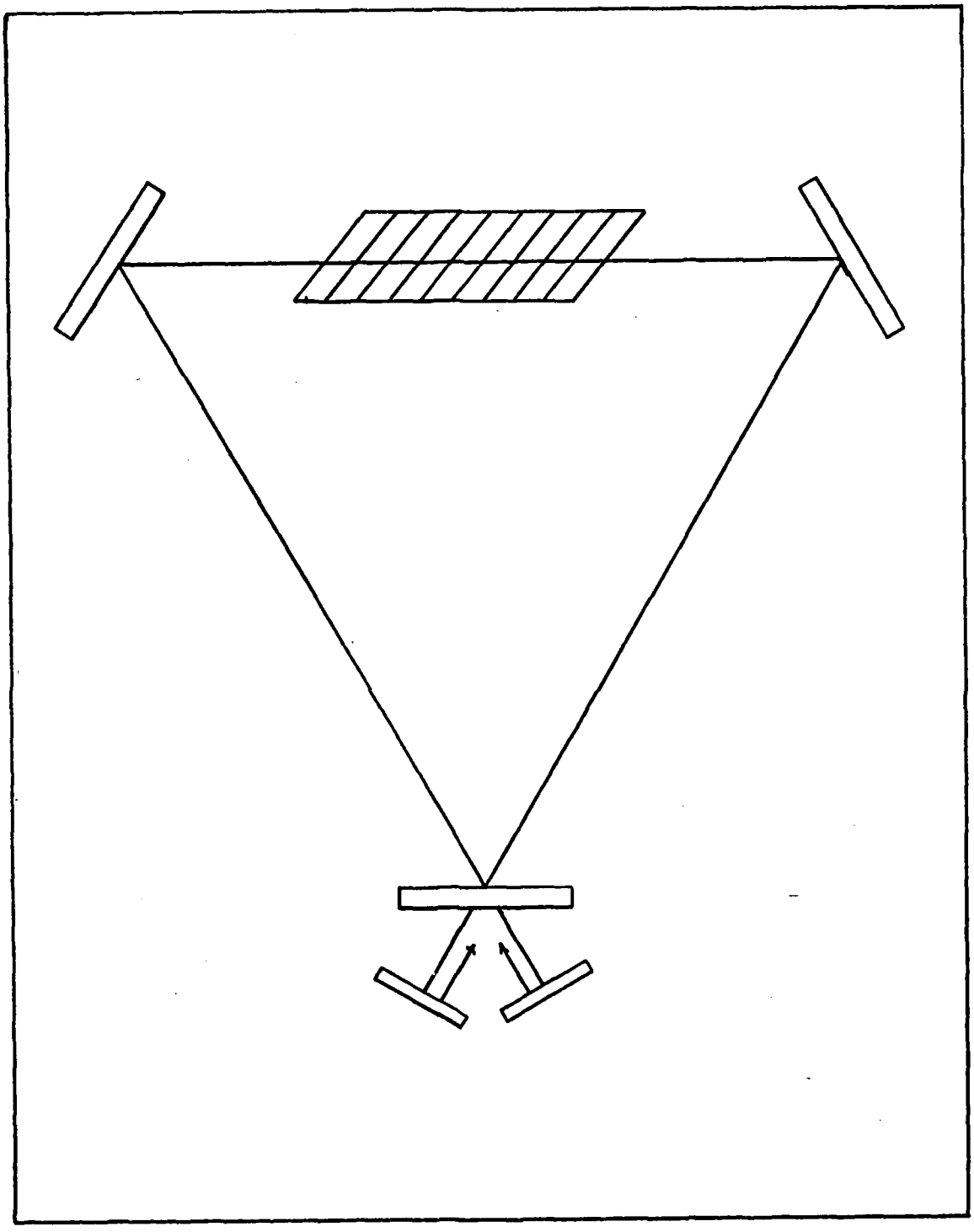

Figure 2.14 Placement of External Mirrors to Provide Mode Competition

reduction in the available gain, the CW beam will be extinguished. The same will occur to the CCW beam.

To use this effect to cause beam alternation, it is necessary to alternately block the reflected beams. The following sections will discuss means of accomplishing this.

Mechanical Chopper

The simplest way of alternately blocking the reflected beams is the use of a mechanical chopper. The chopper must be designed such that it never blocks nor passes the two reflected beams simultaneously. As can be seen in Figure 2.15, this is achieved by ensuring that the angular separation between the two beams is an odd multiple of the spaces in the chopper. For this discussion, the angular separation is 180 degrees, or three times the blade angles of 60 degrees.

By rotating the chopper through the beams passing from the cavity to the external mirrors, the CW and CCW beams are alternately extinguished, as in Figure 2.15. The chopper is a good method due to its simplicity, but may suffer degradation of results due to mechanical and/or acoustical noise.

Electro-optical Shutter

The other arrangement considered for alternating the reflected beams is to use an electro-optic device such as a Kerr cell to act as a shutter on the reflected beams.

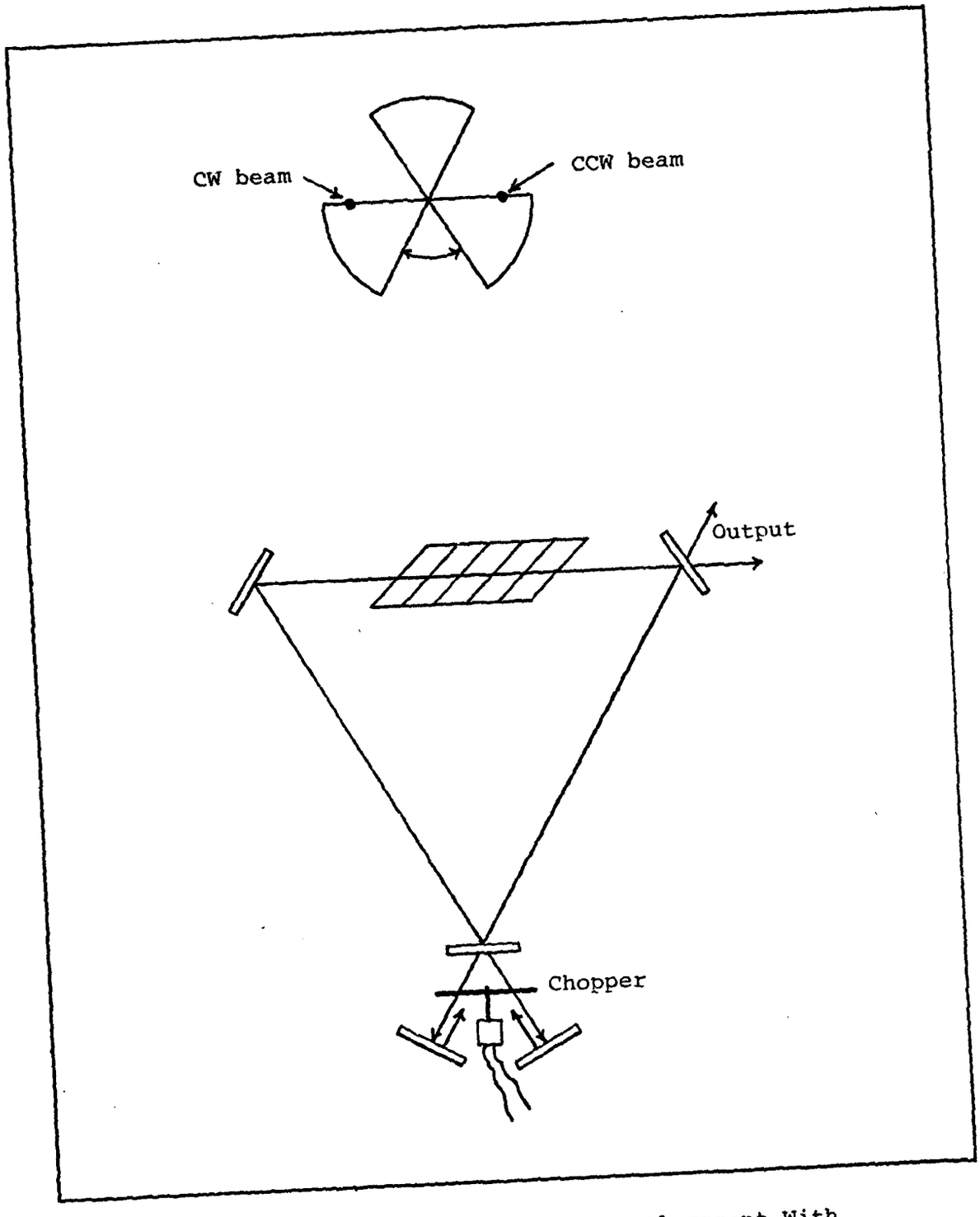

Figure 2.15 Optical Chopper and its Placement With Respect to the Laser Cavity

The Kerr cell makes use of the Kerr electro-optic effect (not to be confused with the Kerr magneto-optic effect mentioned earlier). This is a quadratic effect which may be induced by an electric field in many solids and liquids. When light is propagated at right angles to the electric field, induced birefringence causes an optical phase difference

$$\phi = \frac{2\pi}{\lambda} (n_e - n_o) \, l \qquad (2.13)$$

with l the geometrical path length in the direction of propagation and n_e and n_o are again the refractive indices of the extraordinary and ordinary waves. Field strength E^2 , and optical difference ϕ are related by

$$\phi = 2\pi K E^2 \, l \qquad (2.14)$$

where K is the Kerr constant (a function of temperature and wavelength). For $\phi = \pi$ rad, the half-wave cell voltage is found by

$$\phi = \pi = 2\pi K E^2 l \qquad (2.15)$$

Solving this for E

$$E = \frac{1}{\sqrt{2Kl}} \qquad (2.16)$$

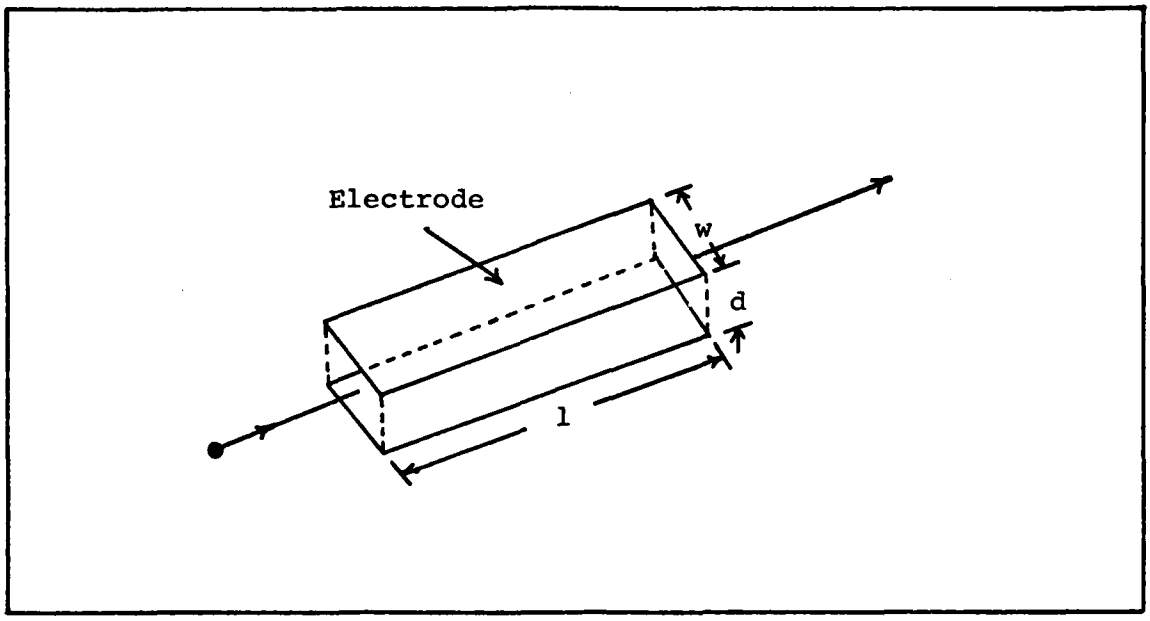

Figure 2.16 Parallel Plate Kerr Cell Geometry

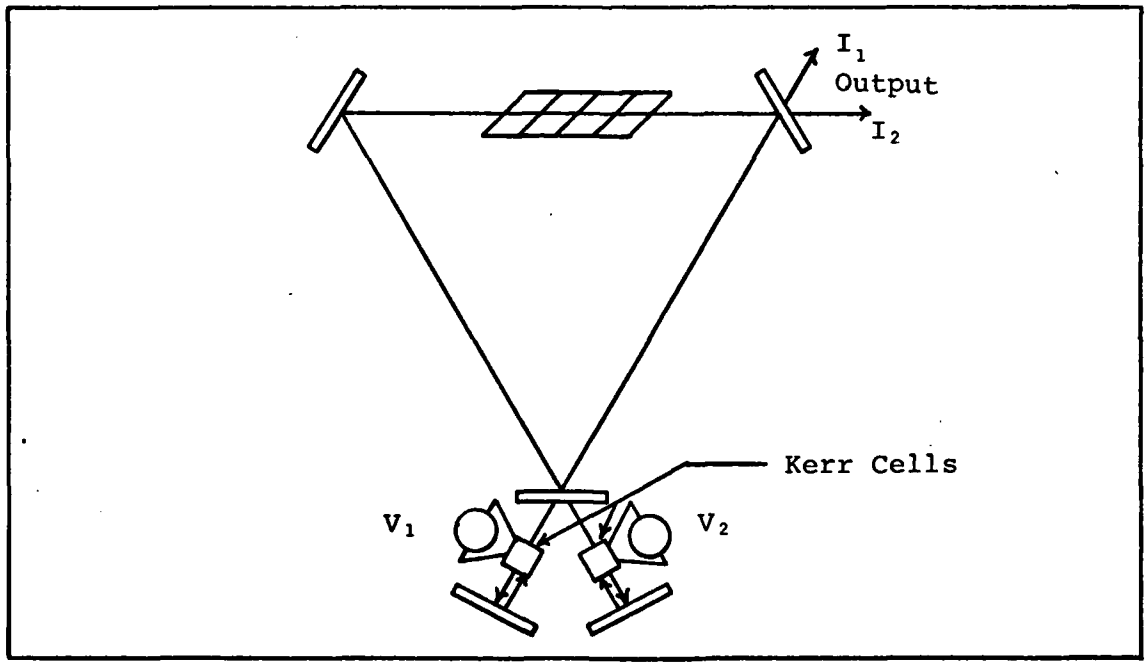

Figure 2.17 Placement With Respect to Laser Cavity

V_s is then related to E by $E = V_s/d$ (see Figure 2.16). Substituting V_s/d for E in Eq 2.16 gives the following relationship for the half-wave cell voltage

$$V_{\lambda/2} = \frac{d}{\sqrt{2Kl}} \qquad (2.17)$$

While the Faraday cell was a nonreciprocal device, meaning that plane polarized light traveling in one direction is rotated in the opposite direction from light traveling in the opposite direction, the Kerr cell, like the simple retardation plate, is a reciprocal device. It in fact works as an electrically switchable retardation plate.

When used as a shutter, the Kerr cell is operated at its quarter-wave cell voltage. The plane polarized light beam from the laser cavity is incident upon the Kerr cell with its plane of polarization at a 45 degree angle to the optic axis. After passing through the Kerr cell, the light is right circularly polarized due to the quarter-wave retardation. After reflecting from the external mirror, the beam passes through the Kerr cell once again, and is again retarded by a quarter-wave, for a total phase retardation of one half-wave. This results in the plane of polarization being oriented at an angle of 45 degrees on the opposite side of the optic axis from the original plane of polarization, for a rotation in the plane of

polarization of 90 degrees. Thus if the beam had been vertically polarized because of the Brewster window when it left the cavity, it would reenter the cavity horizontally polarized. Thus it is unable to enter the gain tube, and mode competition does not occur. With two Kerr cells placed as shown in Figure 2.17, beam alternation may be achieved by applying square waves that are 180 degrees out of phase with each other to the two Kerr cells (Figure 2.18).

The Kerr cell is a capacitive element, thus the electrical circuit including the Kerr cell is shown in Figure 2.19. The voltage-ratio transfer function for this network is

$$\frac{V_2}{V_1} = \frac{Z_2}{Z_1 + Z_2} = \frac{\frac{1}{j\omega C}}{\frac{1}{j\omega C} + R} = \frac{\frac{1}{RC}}{j\omega + \frac{1}{RC}} \qquad (2.18)$$

The asymptotic values of magnitude and phase can be determined by inspection of Eq 2.18. For small ω, the magnitude is approximately 1 and the phase is 0 degrees. For large ω, the magnitude approaches 0 while the phase angle becomes approximately 90 degrees. This produces a frequency response which is shown in Figure 2.19.

For example, assume a Kerr cell with a capacitance of 100 pf and a voltage source with an output resistance of 50 Ω. The half power point, 1/RC, is thus at 31.831 MHz.

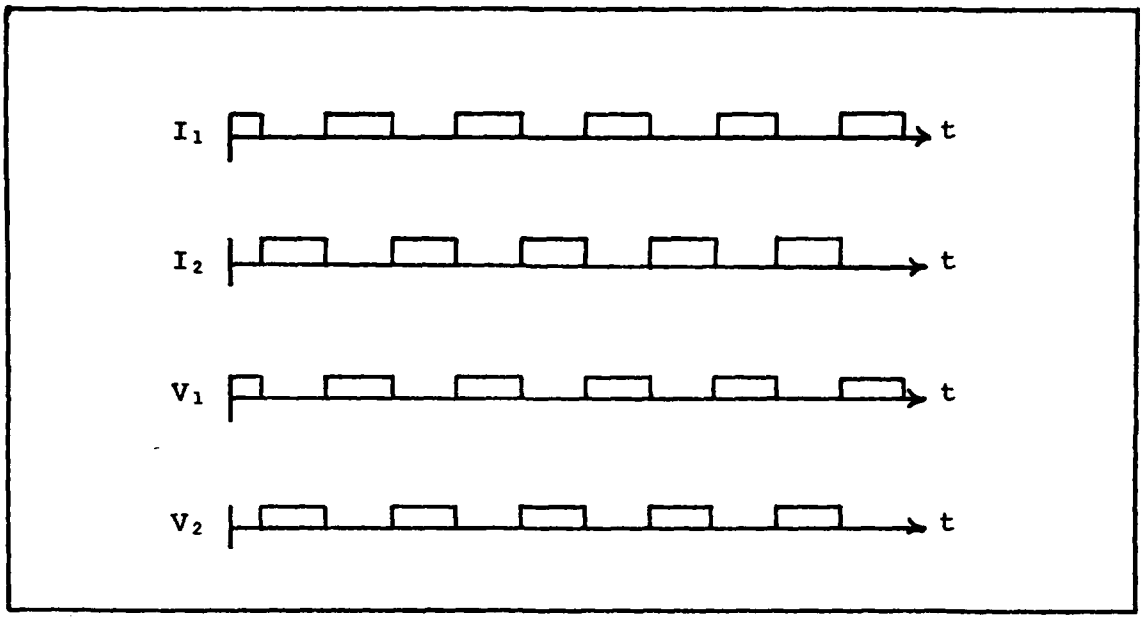

Figure 2.18 Kerr Cell Voltage and Laser Output

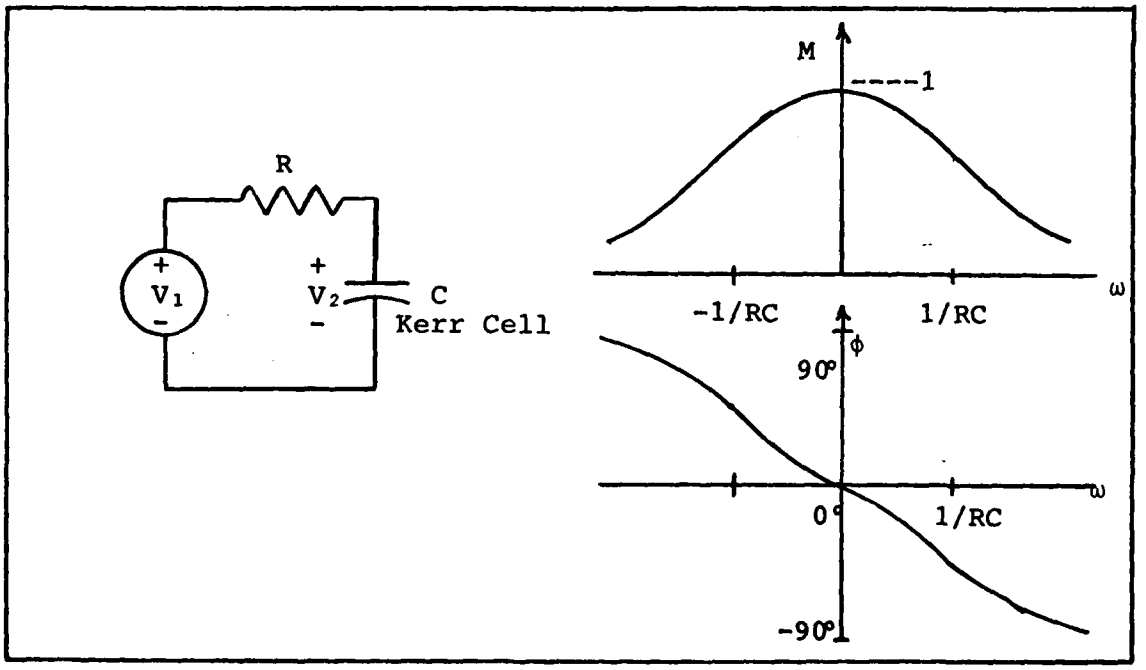

Figure 2.19 Kerr Cell Circuit and Frequency Response

III. Design of Equipment

Ring Laser

A diagram of the laser is shown in Figure 3.1. The laser cavity is made up of three aluminum mirror mounts and a laser gain tube support. The gain tube support consists of two carbon steel end plates, four super-invar rods as spacer bars, and two carbon steel support blocks to hold the laser gain tube in place. The laser mirrors are secured in their mounting blocks by aluminum tabs which are screwed to the mounting blocks. The mounting blocks are then attached to the mirror mounts by three sprung screws. Alignment is accomplished with three alignment screws per mount. The laser gain tube support and the mirror mounts are bolted to a bottom plate of .75 inch aluminum and are covered with a top plate of .25 inch aluminum. The cavity perimeter, L (optical distance from the output mirror around the ring back to the output mirror) is equal to 150 cm, $\approx$50 cm to a side. Scale drawings of the laser hardware are included in Appendix A. Figure 3.2 is a picture of the assembled laser and includes the mechanical chopper.

A discussion concerning critical components in the laser design is presented in the following sections.

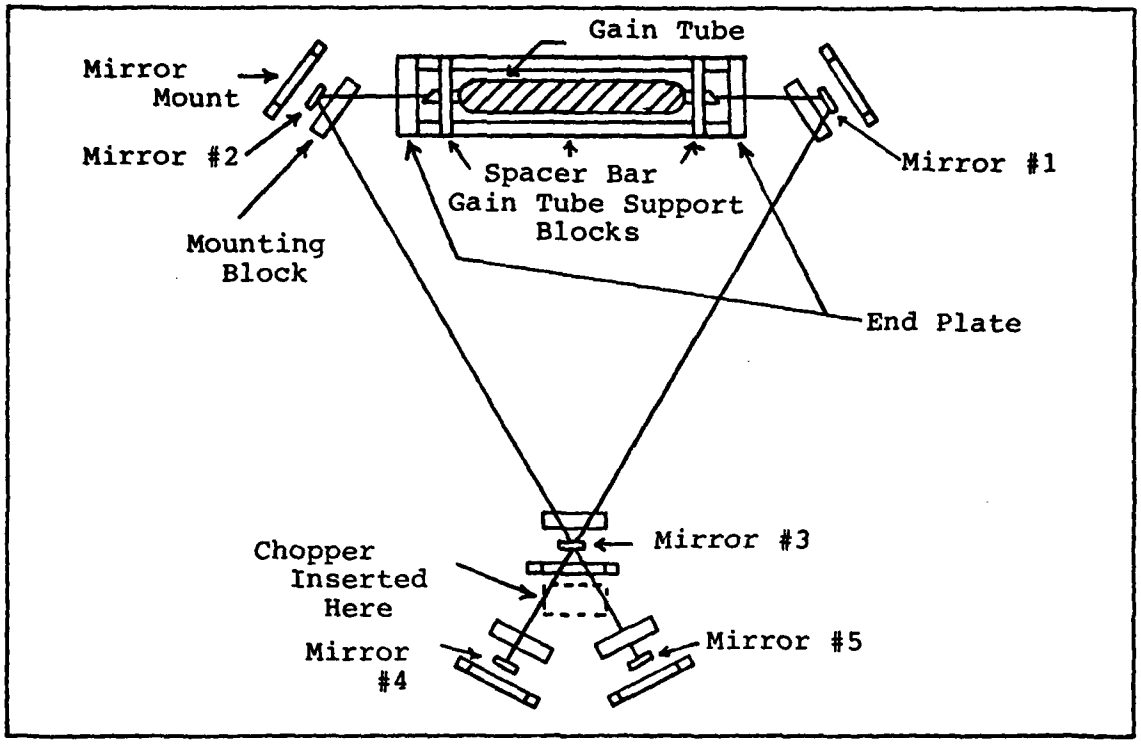

Figure 3.1 Laser Design

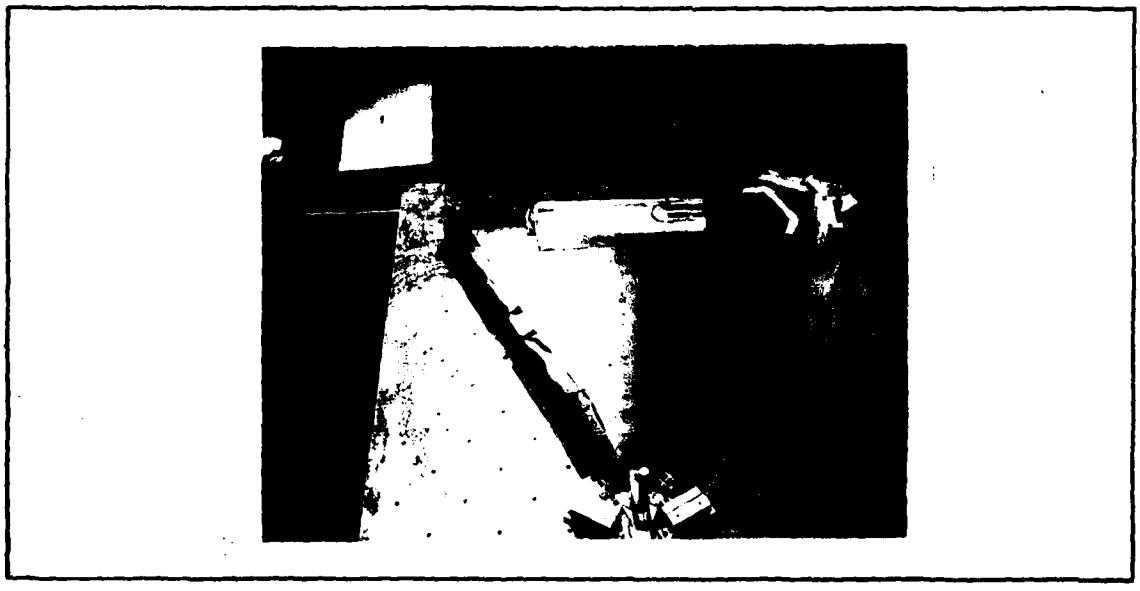

Figure 3.2 Laser Cavity with Mechanical Chopper

Laser Gain Tube

A Spectra-Physics model 120 helium-neon gain tube is used and is pumped by a Spectra-Physics model 249 power supply. The gain tube draws a nominal 6.0 ma and is designed for a 5 mw output.

Laser Mirrors

The laser mirrors were selected in accordance with two criteria. First, the spot size of the beam at the windows of the gain tube, and second, stability criteria.

The spot size at the windows of the gain tube is needed to ensure that enough of the beam to provide lasing is passed through the gain tube. First, the spot size at the center of the tube is calculated, using

$$R = z\left[1 + \left(\frac{\pi\omega_0^2}{\lambda z}\right)^2\right] \qquad (3.1)$$

where R is the radius of curvature of the beam at distance z from the center of the tube (Ref 7:468). The distance desired is the distance from the center of the tube to the mirror at the cavity apex opposite it. For the cavity being designed this distance is 75 cm. A one meter radius mirror is chosen for this position, which gives a calculated spot size at tube center of .295 mm. Taking this value for ω_0, the spot size at the window is calculated from

$$\omega(z)^2 = \omega_0^2 + \frac{\lambda^2 z^2}{\pi^2 \omega_0^2} \qquad (3.2)$$

with z equal this time to 16.75 cm, the distance from the center of the gain tube to the window. $\omega(16.75)$ is found to be 0.3167 mm.

If the laser beam is assumed to be modeled as a Gaussian distribution, the bore of the gain tube must have a diameter of 6σ to permit 99.7% of the beam to pass through the tube. To determine what the 6σ value is, the laser beam field equation

$$\underline{E}(x,y,z,t) = E_o e^{ik(x^2+y^2)/2R(z)} e^{-(x^2+y^2)/\omega^2(z)} \times \left(e^{i(kz+p(z)-\omega t)}\right) \qquad (3.3)$$

is set equal to the normal distribution function

$$f_x(x) = \frac{1}{\sqrt{2\pi}\sigma} e^{-\frac{1}{2}\frac{(x-\mu)^2}{\sigma^2}} \qquad (3.4)$$

This is done by setting the imaginary coefficients of the field equation equal to zero and letting

$$E_o = \frac{1}{\sqrt{2\pi}\sigma}$$

This leaves

$$e^{-\frac{x^2+y^2}{\omega^2(z)}} = e^{-\frac{1}{2}\frac{(x^2-\mu^2)}{\sigma^2}}$$

Solving for σ, we get

$$\sigma = \frac{\omega(z)}{\sqrt{2}} \tag{3.5}$$

When the calculated value for $\omega(z)$ is used, the 6σ value is found to be 1.343 mm. Since the bore diameter of the gain tube is 1.5 mm, it will thus pass more than 99.7% of the beam.

The other criterion which the cavity must satisfy is the stability criterion. Looking at Figure 3.3, a schematic of the laser cavity is presented. With it is shown a biperiodic lens system which is its equivalent, with f_i equal to $R_i'/2$ (Ref 9:71). R_i' is the radius of curvature corrected for an angle of incidence other than the normal to the mirror surface, due to astigmatism. The two corrections are

$$R_i' = R_i \cos\Theta \tag{3.6a}$$

and

$$R_i' = R_i/\cos\Theta \tag{3.6b}$$

where Θ is the angle of incidence. The radii, corrected radii and focal lengths for the equivalent lens system are given in Table 3.1.

		Case 1		Case 2	
i	R_i (m)	R_i (m)	f_i (m)	R_i (m)	f_i (m)
1	5	5.77	2.89	4.33	2.17
2	∞	∞	∞	∞	∞
3	1	1.15	.575	.866	.433

Table 3.1 Radii of Curvature for Cavity Mirrors and Focal Lengths of Model Lenses

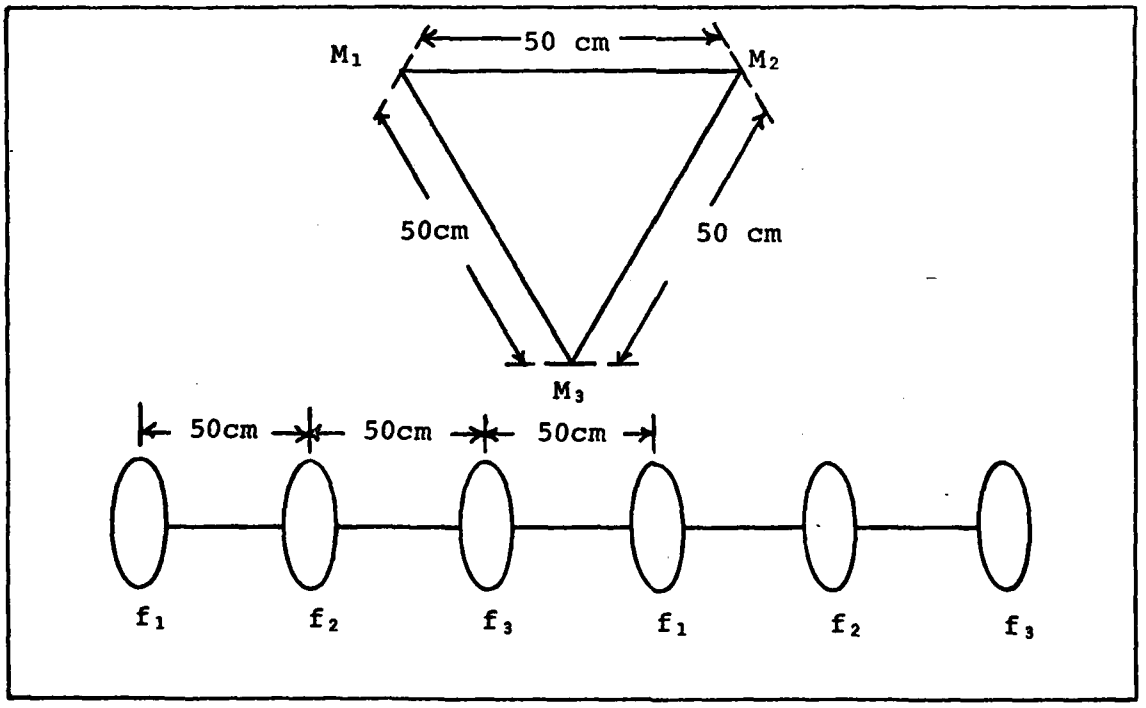

Figure 3.3 Ring Laser Cavity and Biperiodic Lens System Equivalent

Using this model, the stability criterion is applied to the lens system. For stability

$$0 < g_1 g_2 \ldots g_n < 1 \tag{3.7}$$

where the g's are the g-parameters of the lens system. The lens system g-parameters are

$$g_i = 1 - \frac{d}{2f_i} \tag{3.8}$$

(Ref 9:23). Thus for this cavity, the stability criterion is

$$0 < g_1 g_2 g_3 < 1 \tag{3.9}$$

Using the values of f for Case One, the criterion is

$$g_1 g_2 g_3 = (1 - \frac{.5}{5.77})(1 - \frac{.5}{\infty})(1 - \frac{.5}{1.15}) = .516$$

Eq (3.9) then becomes

$$0 \leq .516 \leq 1$$

For Case Two

$$g_1 g_2 g_3 = (1 - \frac{.5}{.433})(1 - \frac{.5}{\infty})(1 - \frac{.5}{.866}) = .374$$

with Eq (3.9) becoming

$$0 \leq .374 \leq 1$$

Both cases meet the stability criterion, and a stable cavity is assured.

With a stable cavity achieved, the dimensions of the beam at various points around the cavity may be calculated. This is done by using Eq (3.2) for a number of points measured from the center of the gain tube. The results of the calculations are listed in Table 3.2.

Mechanical Chopper

The mechanical chopper is a wheel with three 60 degree blades and three 60 degree spaces. It is aligned such that its center is on a line with the two beams after they exit the cavity through the output mirror opposite the gain tube, and so that the blades will interrupt the beams emerging from the cavity. The chopper blade and permanent magnet motor which turns it are mounted on a 0.5 inch diameter aluminum rod to allow them to be adjusted to the correct height. Detailed drawings are contained in Appendix A.

Table 3.2

Beam Diameter as a Function of Distance From Center of Gain Tube

z (cm)	ω(z) (μm)	z (cm)	ω(z) (μm)
0	295.0	40	402.1
5	297.0	45	426.0
10	302.8	50	451.3
15	312.3	55	477.6
20	325.1	60	504.9
25	340.9	65	533.0
30	359.2	70	561.8
35	379.7	75	591.1

IV Experiment and Results

Introduction

After the laser cavity was designed and built, it was necessary that it be aligned. This was done by use of an external alignment laser which was placed such that its beam entered the cavity through the mirror at the apex of the cavity farthest from the gain tube. The beam was then aligned by means of adjustment screws on the alignment laser mount and the mirror to the right of the gain tube so that it was able to pass through the gain tube without reflection from the gain tube walls. The beam was then reflected from the mirror at the left end of the gain tube so that it struck the mirror through which the beam entered the cavity at the point of entry. This mirror was then adjusted so that the entering beam and the reflected beam struck the mirror on the left end of the gain tube at the same point.

Following the use of the alignment laser, the gain tube was energized, and small adjustments were made to the apex mirror until lasing was detected. The three cavity mirrors were then adjusted so as to peak the output intensity of the laser.

After the peaking of the laser output, the external mirrors were adjusted to reflect the output beams back into the gain tube by obtaining a decrease in the output intensity.

The mechanical chopper was then installed and aligned such that it passed one beam while blocking the other.

Experiment 1

The purpose of the first experiment is to establish the detector noise level and the normal output level of the laser. This is done with the external mirrors covered. Figure 4.1 shows the results of this experiment. At time t = 0 seconds, the detectors for both output beams are covered. The only output is thus the detector noise, which is approximately 4.7 μWatts for each detector. At t = 10.5 seconds, the A beam detector is uncovered, resulting in beam intensity of approximately 34.5 μWatts. The A beam detector is recovered at t = 20.5 seconds and the B beam detector is uncovered at t = 23.3 seconds. The B beam is approximately 36.1 μWatts. The B beam is then recovered at t = 34 seconds.

Experiment 2

The purpose of Experiment 2 is to establish the output level of the laser with the external mirrors reflecting the beams back into the cavity. In Figure 4.2, the results of this experiment for the A beam are shown. At t = 0 seconds, the external mirror is blocked so that the output is the laser's normal 34.5 μWatts. At t = 18 seconds, the external mirror is allowed to reflect the A beam back into the cavity.

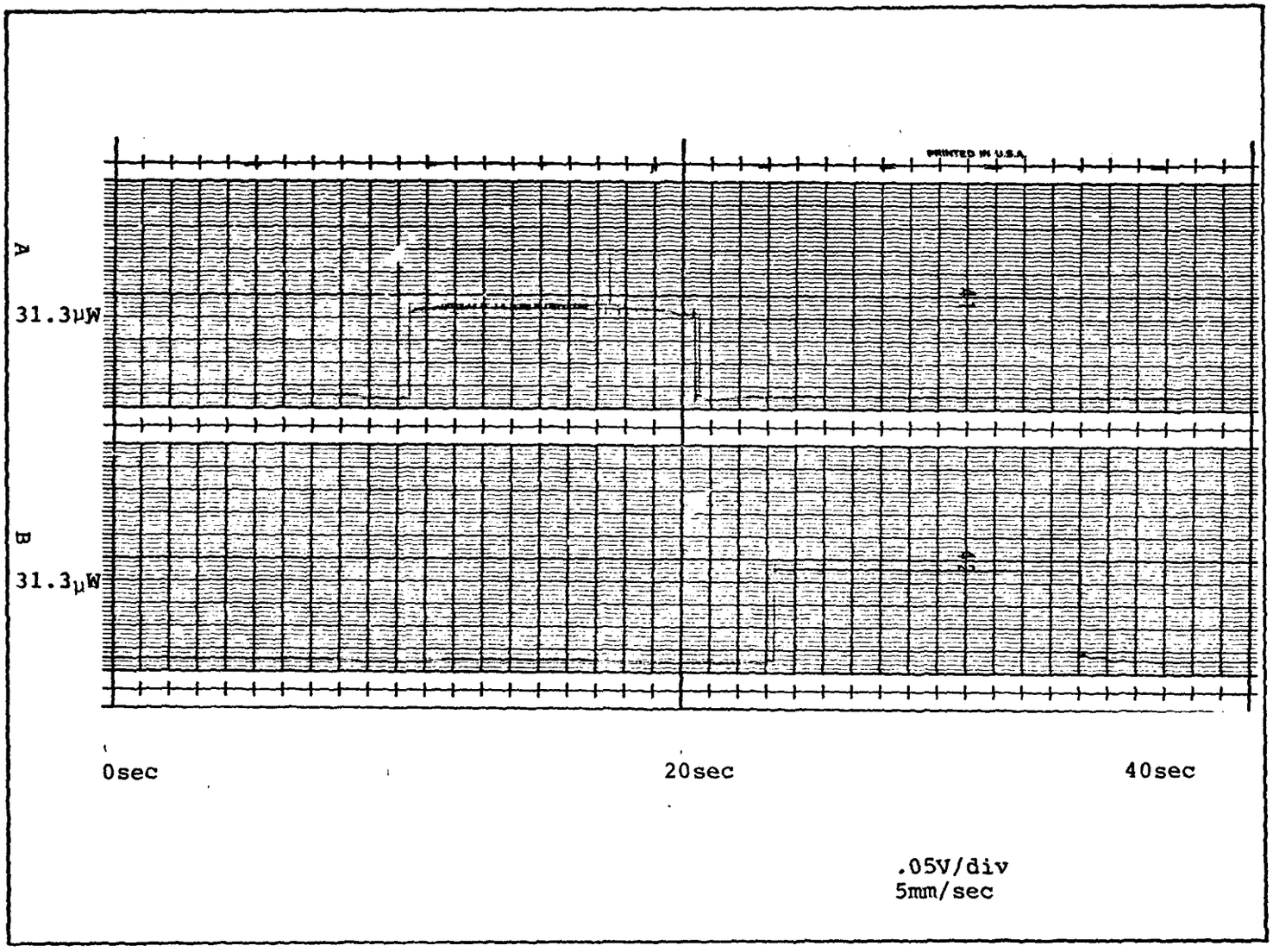

Figure 4.1 Experiment #1 Output

The beam immediately drops to a level of 17.3 μWatts, and by t = 21.5 seconds, the output level has settled to approximately 4.7 μWatts. At t = 28.4 seconds, the A beam detector is blocked, and a detector noise output of 1.6 μWatts is seen.

Figure 4.3 shows the experiment repeated for the B beam. At t = 0 seconds, with the B beam external mirror covered, the laser output intensity is 34.5 μWatts. At t = 11.4 seconds, the mirror is uncovered and the output level drops to approximately 12.6 μWatts. The B beam detector is covered at t = 20.8 seconds, and a detector noise level of 1.6 μWatts is seen.

Experiment 3

The purpose of Experiment 3 is to inspect the output of the laser with the mechanical chopper in operation. The results are shown in Figure 4.4. The chopper is causing the beams to alternate at a 465.1 Hz rate. It can be seen that the beams do not switch simultaneously. This is due to misalignment in the chopper rotor. Because of this misalignment, there is a period of approximately .2 msec where the beams are simultaneously off or on.

The effects of coupling between the two beams may also be seen. During the first cycle shown in Figure 4.4, when the A beam is high and the B beam is low, the A beam intensity is approximately 62.7 μW and the B beam intensity is approximately 12.6 μW. During the second cycle, again with A

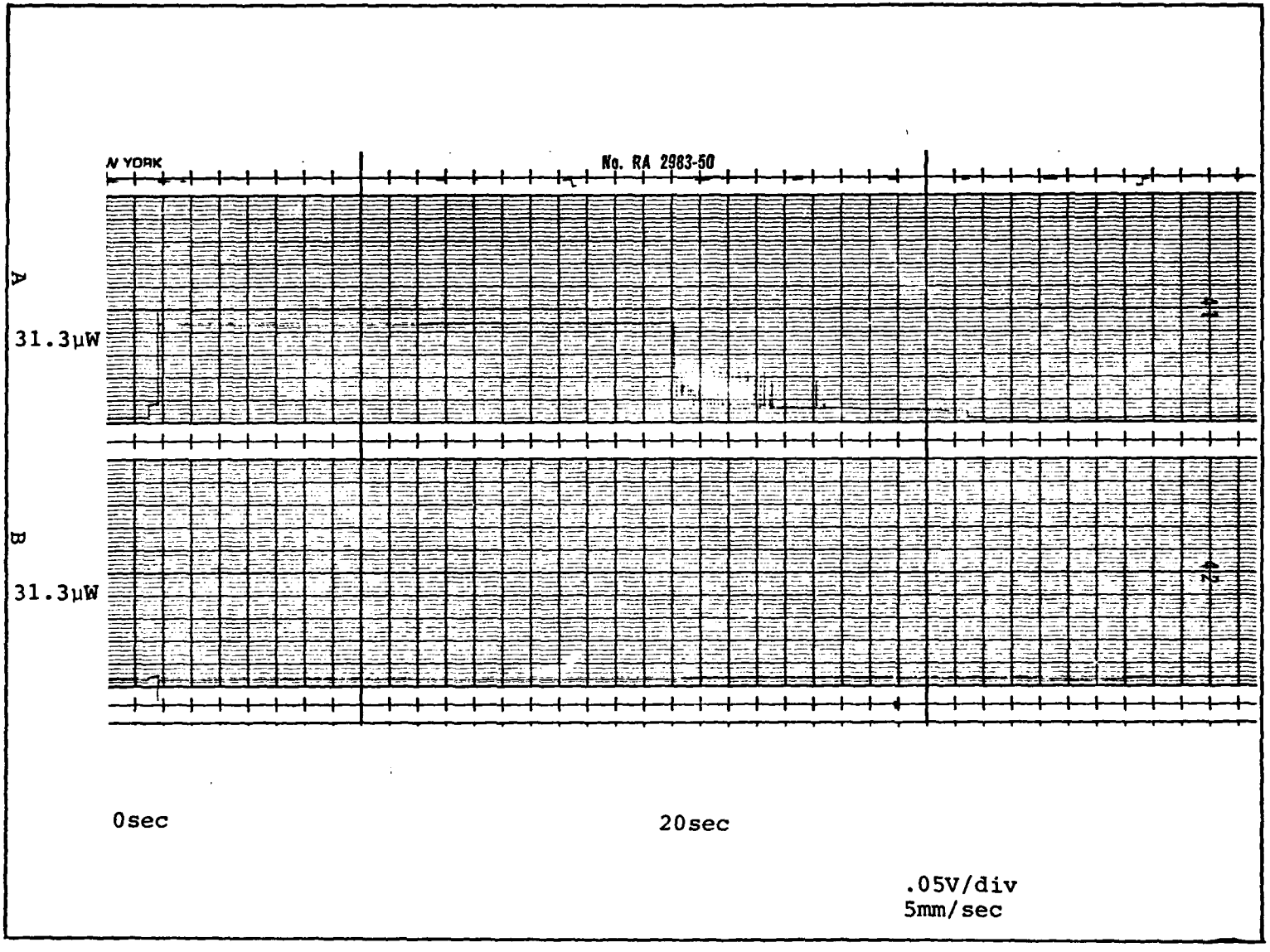

Figure 4.2 Experiment #2 A Beam Output

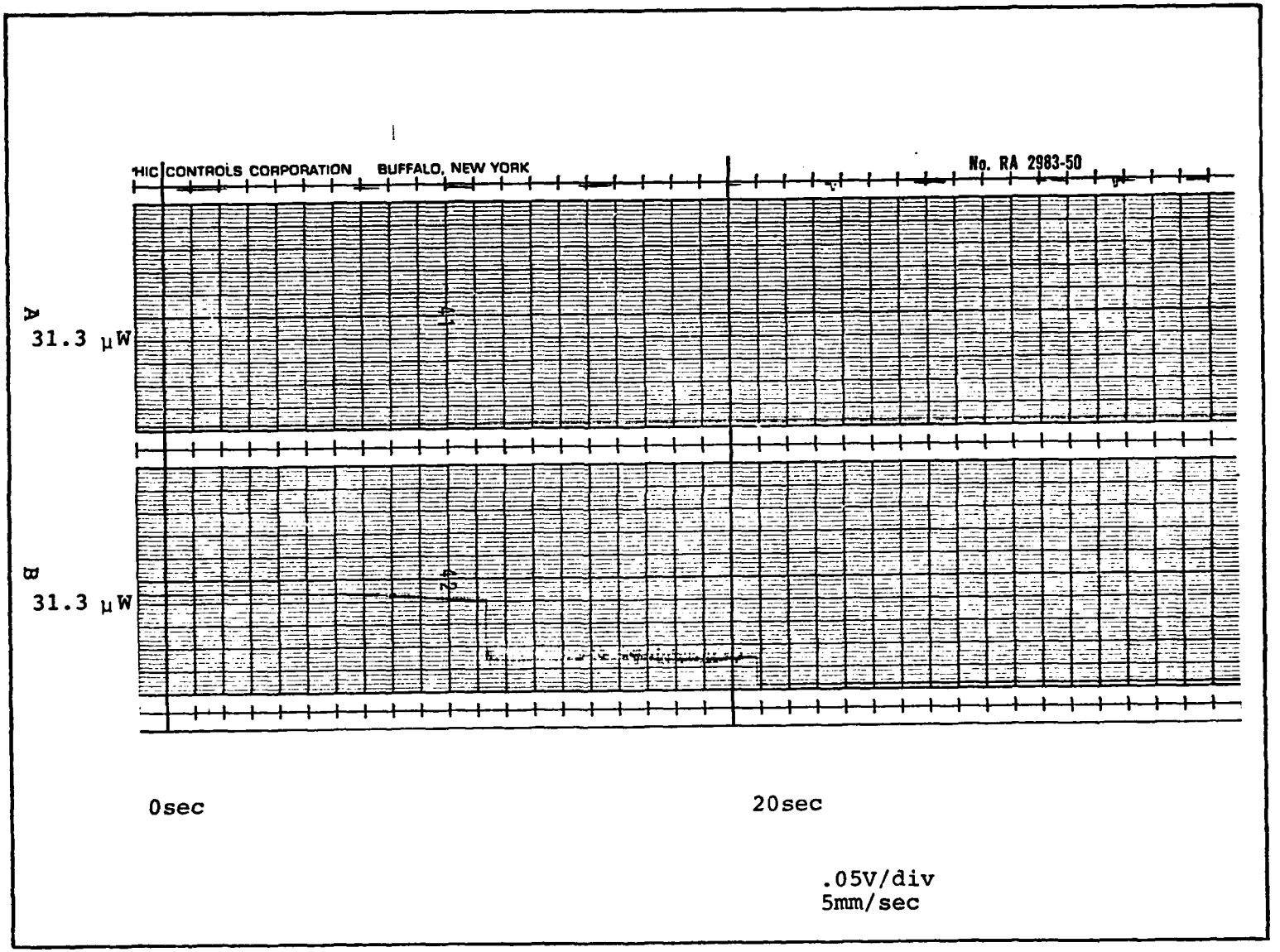

Figure 4.3 Experiment #2 B Beam Output

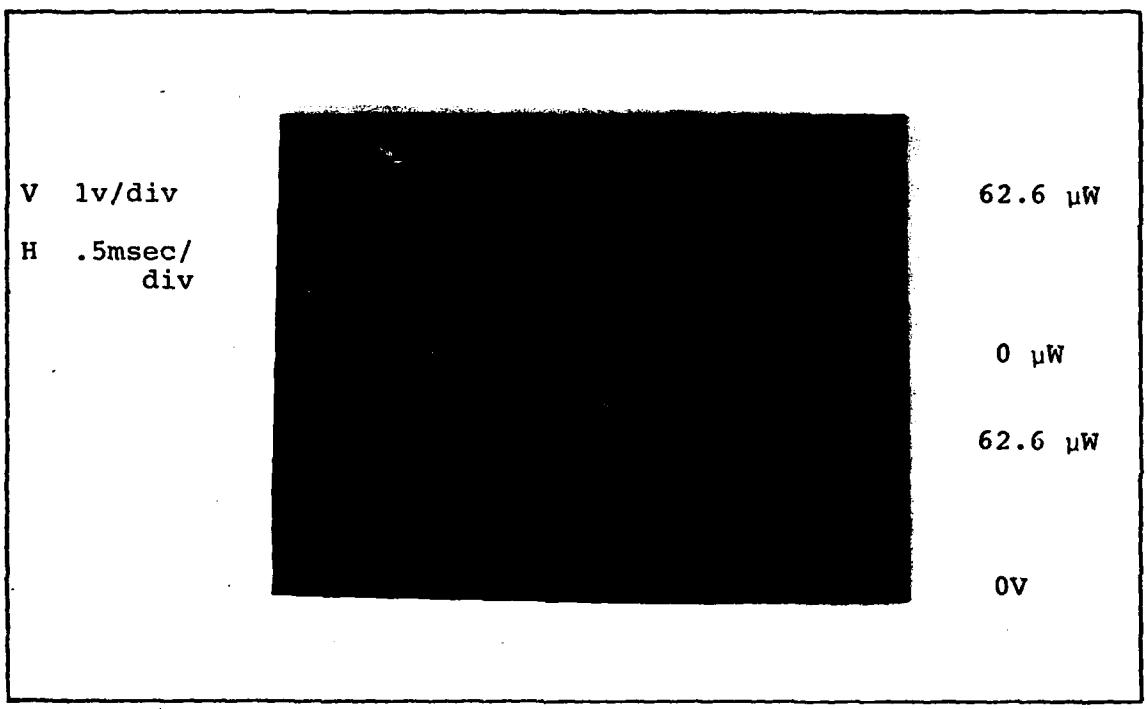

Figure 4.4 Experiment #3 Output

high and B low, the A beam output has risen to approximately 72.2 μW and the B beam output has risen to approximately 3.1 μW. The rise in A and the decrease in B are both 9.4 μW, indicating that the beams are coupled together. This is due to backscatter from the mirrors. While some backscatter is inherent in any mirror, it may also arise from imperfections in the surface of the mirror, such as dust particles or scratches.

The switching speed of the beam is of course determined by the rotation rate of the chopper. For this chopper, three cycles are obtained per one rotation of the rotor. This results in a rotational rate in RPM that is 20 times the switching frequency. Thus for the waveform of Figure 4.4, the switching frequency of 465.1 Hz is the result of rotating the chopper at 9302 RPM.

Lastly, the ringing which may be seen on the detector output is caused by the response of the detector amplifier circuit to the switching of the beams. The ringing frequency of approximately 30 KHz is a function of the input capacitance of the amplifier and the feedback resistance.

V Conclusions and Recommendations

Conclusions

As was stated in Chapter I, the purpose of this research was to investigate the feasibility of alternating beams in a ring laser by three methods. The results of Chapter IV have demonstrated that the second of these methods, mode competition and a mechanical chopper, is indeed feasible.

The analysis of the two other methods, the Faraday cell optical switch and mode competition with an electro-optic shutter, shows that they too are feasible. Both have the desireable characteristics of no moving parts, and both warrant experimental investigation.

Recommendations regarding further research into the mechanical chopper method, and initial experimental investigation into the Faraday cell switch and the electro-optic shutter are contained in the following section.

Recommendations

It is recommended that the two methods which were not demonstrated experimentally be tested. Along with the demonstration of these two methods, performance comparisons of all three methods investigated in this research should be done.

Following the testing of the Faraday cell and electro-optic shutter methods, research into the application of

the three methods investigated to the solution of the active ring laser gyroscope lock-in problem should be done. The effect of switching speed on gyroscope operation should also be investigated. Should higher switching speed be desired from the mechanical chopper method, the number of blades can be increased until the width of the blades is equal to the spot size of the beam.

Bibliography

1. Aplet, L.J. and J.W. Carson. "A Faraday Effect Optical Isolator," Applied Optics, 3: 544-545 (April 1964).

2. Aronowitz, Frederick. "The Laser Gyro," Laser Applications, edited by Monte Ross. New York: Academic Press, 1971.

3. Bennet, J.M. and H.E. Bennet. "Polarization," Handbook of Optics, edited by W.G. Driscoll. New York: McGraw-Hill Book Company, 1978.

4. Chen, Di. "Magneto-Optic Principles, Materials and Applications," Proceedings of the Society of Photo-Optical Instrumentation Engineers, 9-15. Boston, Massachusetts: May 1973.

5. Gensic, J.E. and H.E.D. Scovill. "A Unidirectional Traveling Wave Optical Maser," Bell System Technical Journal, 41: 1371 (1962).

6. Hartfield, Edward and B.J. Thompson. "Optical Modulators," Handbook of Optics, edited by W.G. Driscoll. New York: McGraw-Hill Book Company, 1978.

7. Kogelnik, Herwig. "Imaging of Optical Modes-Resonators with Internal Lenses," Bell System Technical Journal, 44: 455-494 (1965).

8. O'Shea, Donald C., W. Russel Callen, and William T. Rhodes, Introduction to Lasers and Their Applications. Massachusetts: Addison-Wesley Publishing Company, 1977.

9. Yariv, Amnon. Introduction to Optical Electronics, 2nd ed. New York: Holt, Rinehart and Winston, 1976.

Appendix A Laser Hardware Designs

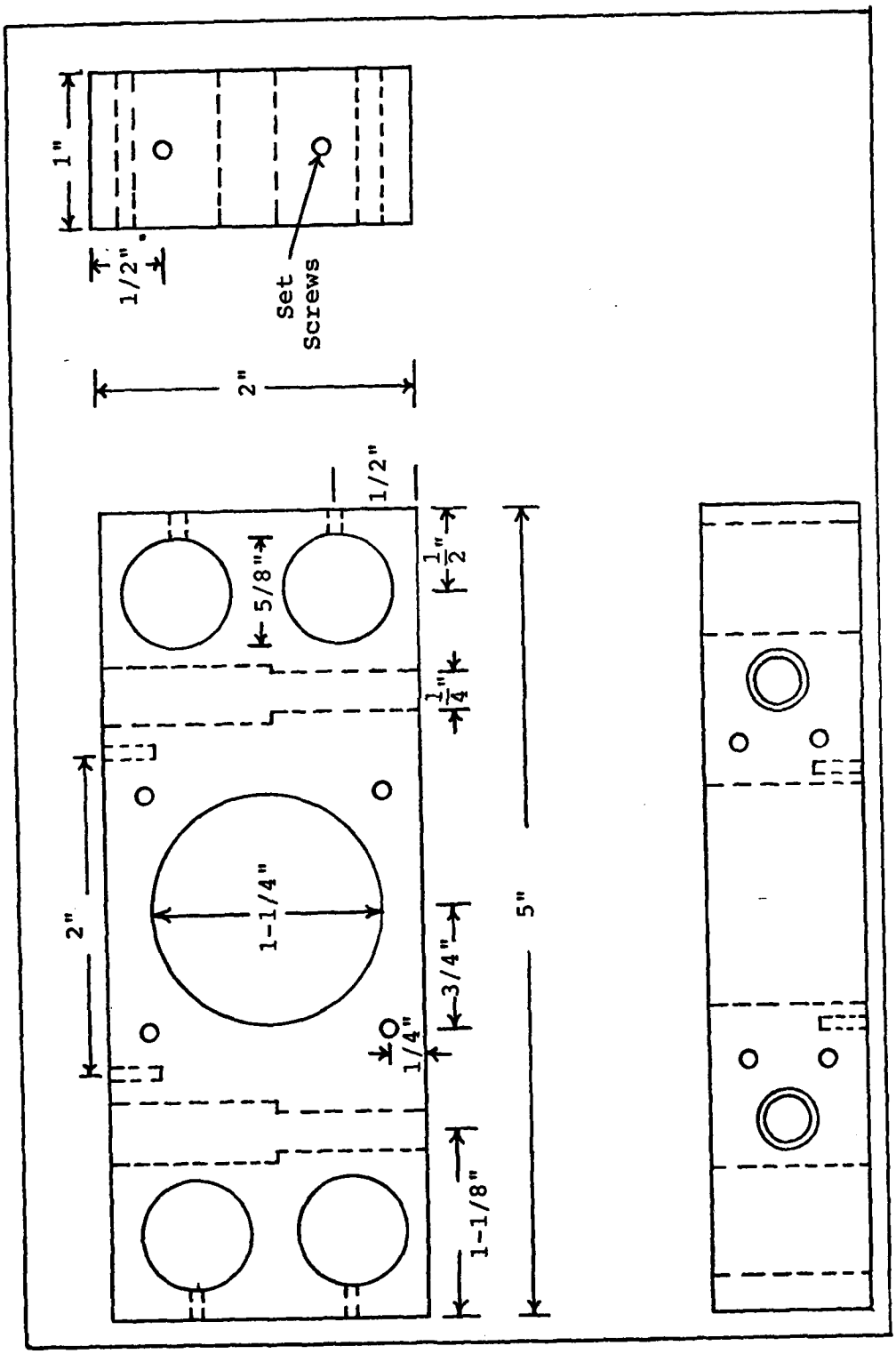

Figure A.1 Laser End Plates

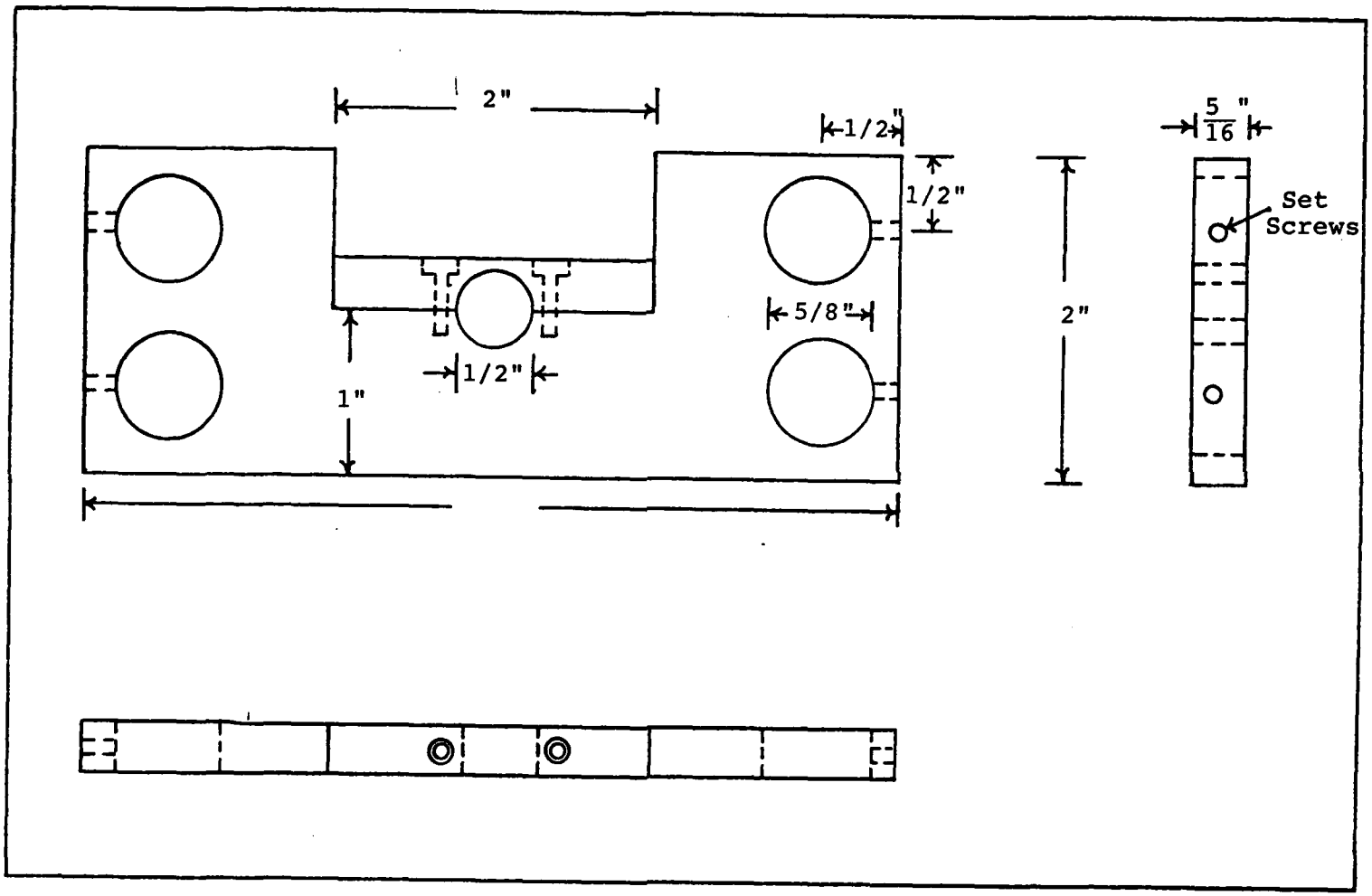

Figure A.2 Laser Gain Tube Support Blocks

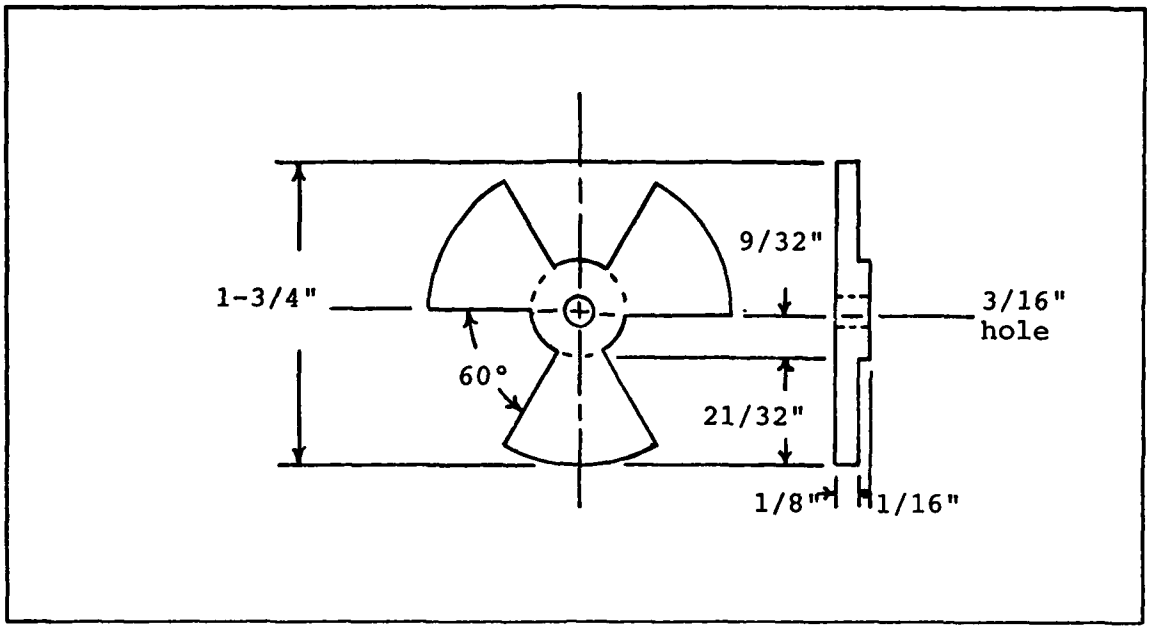

Figure A.3 Chopper Blade

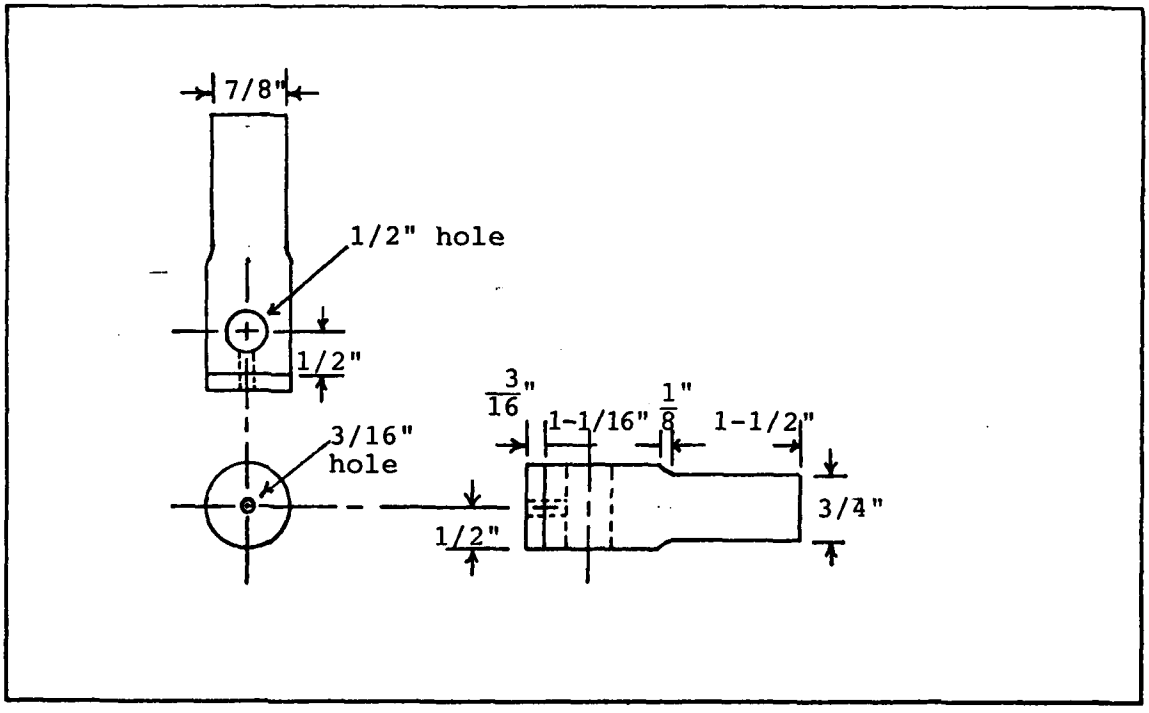

Figure A.4 Chopper Motor Mount

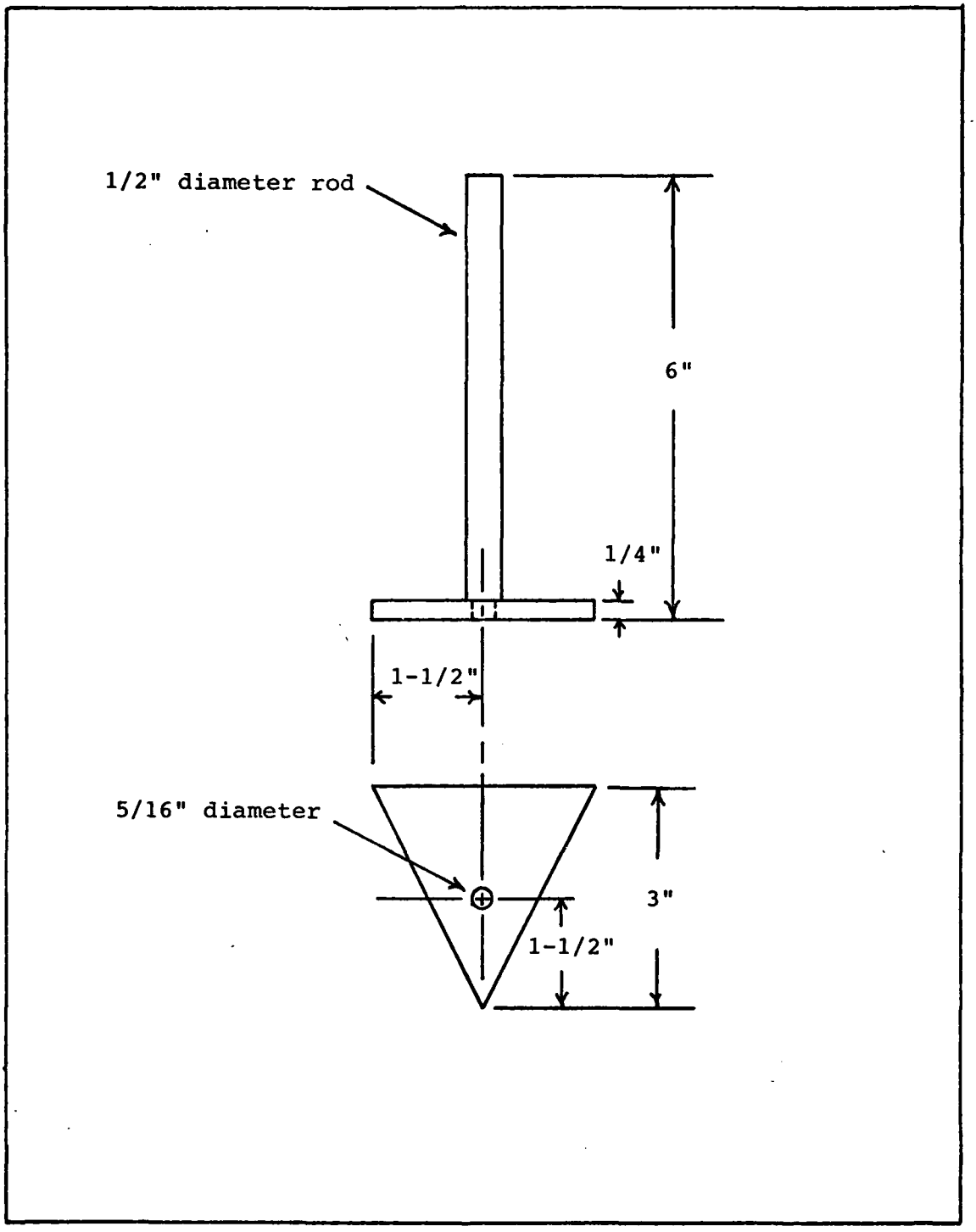

Figure A.5 Chopper Stand

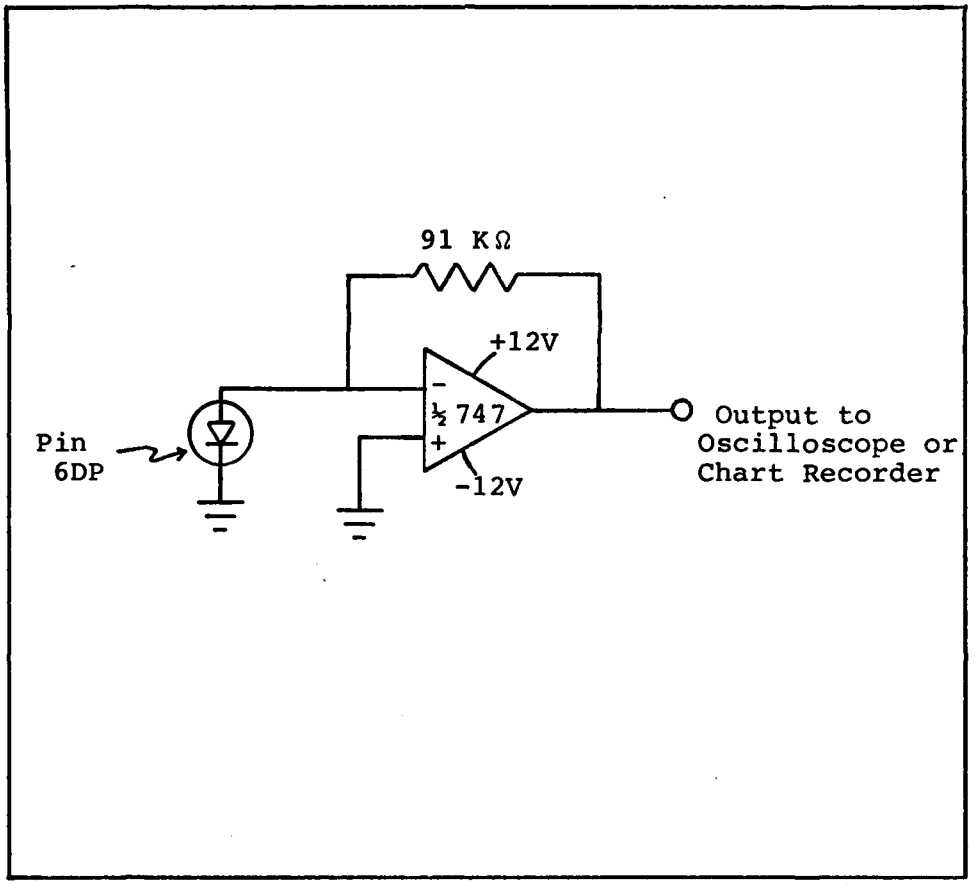

Figure A.6 Photodetector Circuit

Appendix B Equipment List

2 - Hewlett-Packard 6236B Triple Output Power Supplies

1 - Tektronics 565 Dual Beam Oscilloscope

2 - Tektronics 3A75 Amplifiers

1 - Gould Brush 200 Chart Recorder

1 - Tektronics C-30 Scope Camera

1 - Strombeck DC Permanent Magnet Motor

VITA

Marc L. Drake was born on 5 April 1952 in Jamestown, New York. He graduated from Newfane, New York Central High School in 1970, and entered Niagara University three months later. In January 1973 he enlisted in the United States Air Force. He received an Associate of Arts degree from the University of Maryland in 1977. He graduated from Ohio University in June 1980, with a Bachelor of Science degree in Electrical Engineering, and received his commission from the Reserve Officers Training Corps. He entered the School of Engineering, Air Force Institute of Technology later that month and pursued studies towards a Master of Science degree in Electrical Engineering. Lieutenant Drake is scheduled to be assigned to the Ballistic Missile Office at Norton AFB, California upon completion of his studies.

UNCLASSIFIED

SECURITY CLASSIFICATION OF THIS PAGE (When Data Entered)

REPORT DOCUMENTATION PAGE		READ INSTRUCTIONS BEFORE COMPLETING FORM
1. REPORT NUMBER AFIT/GE/EE/81*D-17	2. GOVT ACCESSION NO. AD-A115 576	3. RECIPIENT'S CATALOG NUMBER
4. TITLE (and Subtitle) METHODS FOR AN ALTERNATING BEAM RING LASER		5. TYPE OF REPORT & PERIOD COVERED MS Thesis 6. PERFORMING ORG. REPORT NUMBER
7. AUTHOR(s) Marc L. Drake 1Lt USAF		8. CONTRACT OR GRANT NUMBER(s)
9. PERFORMING ORGANIZATION NAME AND ADDRESS Air Force Institute of Technology (AFIT/EN) Wright-Patterson AFB, Ohio 45433		10. PROGRAM ELEMENT, PROJECT, TASK AREA & WORK UNIT NUMBERS
11. CONTROLLING OFFICE NAME AND ADDRESS		12. REPORT DATE 15 December 1981 13. NUMBER OF PAGES 71
14. MONITORING AGENCY NAME & ADDRESS(if different from Controlling Office)		15. SECURITY CLASS. (of this report) 15a. DECLASSIFICATION/DOWNGRADING SCHEDULE

16. DISTRIBUTION STATEMENT (of this Report)

Approved for public release; distribution unlimited.

17. DISTRIBUTION STATEMENT (of the abstract entered in Block 20, if different from Report)

15 APR 1982

Dean for Research and Professional Development
Air Force Institute of Technology (ATC)
Wright-Patterson AFB, OH 45433

18. SUPPLEMENTARY NOTES

Approved for public release; IAW AFR 190-17

~~Frederick C. Lynch, Major~~, USAF
~~Director of Public Affairs~~

19. KEY WORDS (Continue on reverse side if necessary and identify by block number)

20. ABSTRACT (Continue on reverse side if necessary and identify by block number)

The purpose of this research is to investigate the feasibility of three methods of alternating beams in ring lasers. The first method is the use of a Faraday cell and a half-wave plate inside the laser cavity to rotate the plane of polarization of one of the counter-rotating beams so that lasing in that direction is not supported. The second method,

DD FORM 1 JAN 73 1473 EDITION OF 1 NOV 65 IS OBSOLETE

UNCLASSIFIED

SECURITY CLASSIFICATION OF THIS PAGE (When Data Entered)

and the one investigated experimentally, is the use of mirrors and a mechanical chopper external to the laser cavity to halt lasing by means of mode competition. The third and final method explored is the replacement of the mechanical chopper with an electro-optical shutter.

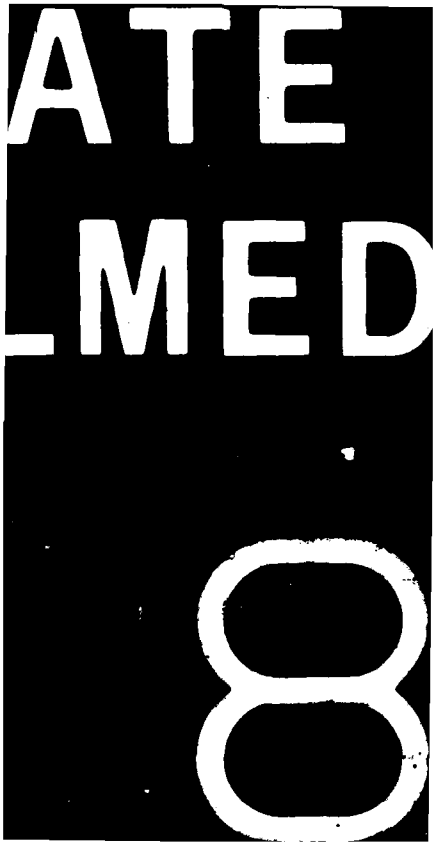
ATE
LMED
8